N° d'ordre :

UNIVERSITE KASDI MERBAH OUARGLA
FACULTE DES MATHEMATIQUES
ET DES SCIENCES DE LA MATIERE
DEPARTEMENT DE PHYSIQUE

Mémoire
MASTER ACADEMIQUE
Domaine : Sciences de la Matière
Filière : Physique
Spécialité : Physique des Rayonnements

Présenté par :
TRABELSI Imane et LAKHDARI Meriem

Thème :

Laser welding of metal alloy parts and calculation of losses by radiation, convection and evaporation

Soutenu publiquement
Le : 24 / 06 / 2023

Devant le jury composé de :

Pr BENMEBROUK Lazhar	Prof.	Président	UKM OUARGLA
Dr BALLAH Zakia	MCB	Examinateur	UKM OUARGLA
Pr KHELFAOUI Fethi	Prof.	Rapporteur	UKM OUARGLA

Année Universitaire: 2022/2023

Dedication

To our parents

For their support and encouragement

To our families

May god bless all of them

To our friends

To our colleagues

To everyone helped us in the realization of this work

Imane & Meriem

Acknowledgements

Firstly we are very grateful to ***Pr. Fethi KHELFAOUI****, This work could never has been completed without his support, assistance, and his availability. We appreciate his valuable advices, instructions and encouragement that allowed us to complete this work.*

We also thank the board of examiners: President ***Pr. Lazhar BENMEBROUK****, and Examiner* ***Dr. Zakia BALLAH*** *for their acceptance to judge this work.*

This work was carried out at Laboratory of Radiation, Plasma and Surface Physics (LRPPS). We want to thank all the staff of this laboratory especially PhD student BENCHAA Sayhia.

Finally we like to thank all the members of the ***TRABELSI*** *and* ***LAKHDARI*** *families, mainly those who were present at our important times, especially our dear's parents.*

Index of contents

Dedication	i
Acknowledgements	ii
Index of contents	iii
List of figures	v
List of tables	vii
General introduction	1
Chapter I: Overview of Laser Welding and Heat Sources	4
1. Welding	4
2. Generalities about laser	4
2.1.Components of a laser	4
2.2.Principle of laser generation	5
3. Laser welding	6
3.1. Laser welding mechanisms	6
4. Deep penetration keyhole welding	8
5.Laser Welding types	8
6. Welding Factors	10
7.Conservation equations	11
8. Energies loss in laser welding	12
9. Influence of shielding gases in the welding process	13
10. References	15
Chapter II : Numerical modeling	17
1. Introduction	17
2. Physical phenomenon	18
3. Hypotheses	18
4. Mathematical Model	18
5. Numerical model	19
5.1. Taylor development	19
5.2. Initial condition and boundary conditions	22
5.3. Gauss–Seidel method	23
6. Laser heat source	24
7. Material Properties	25
8. Diagram of the numerical calculation	27
9. Conclusion	29
Chapter III: Results and Discussion	31
1. Introduction	31
2. Profiles of laser source	31
2.1. Heat laser density according z	31
2.2 . Heat laser density according y	32
2.3 . Heat laser density according x	32

3. Profiles of temperature according time 33
4. Profiles of temperature according position 33
4.1 . Temperatures according z 33
4.2 . Temperatures according x and y 34
5. Temperatures according laser beam power 35
6. Effect of thermal properties of the material 37
7. Effect of convection and radiation losses on temperatures 37
8. Estimation of energy losses by evaporation 39
9. Competition between different losses 41
10. The ratio of energy losses to laser beam energy 42
11. Conclusion 43
12. References 44
General conclusion and perspectives 45

Summary

List of figures

Chapter I

Figure I.1: Diagram illustrating fundamental elements of a laser system [1]. 5
Figure I.2: Modes of radiation interaction with matter. 6
Figure I.3: Conduction mode welding and Keyhole mode[3]**.** 7
Figure I.4: Conduction limited welding [4]. 7
Figure I.5: Sketch of laser beam, keyhole and melt pool[5]. 8
Figure I.6: Ishikawa diagram showing the factors affecting the laser weld quality[13]. 11

Chapter II

Figure II.1: Configuration of laser welding and coordinates system. 18
Figure II.2: Geometric model for phase change. 21
Figure II.3 :2D geometric model meshing. 22
Figure II.4 : model meshing of midpoint. 23
Figure II.5: Heat source power density distribution [5]. 25
Figure II.6: Diagram to calculate the temperature. 27

Chapter III

Figure III.1: Heat laser density according z. 31
Figure III.2: Heat laser density according y. 32
Figure III.3: Heat laser density according x. 33
Figure III.4: : Profiles of temperature as function of time, case of temperature depended properties. 33
Figure III.5: Distribution of temperatures according z. 34
Figure III.6: Distribution of temperatures according x. 34
Figure III.7: Distribution of temperatures according y. 35
Figure III.8: Distribution of temperature according x at the weld center for P=1000 W and P=1200 W. 35
Figure III.9: Distribution of temperature according time at the weld center for P=800W P=1000 W and P=1200 W. 36
Figure III.10: Distribution of temperature according time at (x = 0.225 mm, y = 0.225 mm, z=0.18) for P=800W P=1000 W and P=1200 W. 36
Figure III.11: Temperature profile with 1000 W laser power : comparison between constant and temperature depended properties. 37
Figure III.12: The amount of energy lost by convection and radiation according time. 38
Figure III.13 : The amount of energy lost by radiation and convection according time at the weld center. 39

Figure III.14 : The amount of energy lost by evaporation according x at different position (y = 0.00 mm, z = 0.00 mm),(y = 0.25 mm, z = 0.00 mm),(y = 0.50 mm, z=0.00 mm) at t=0.33 ms. 40

Figure III.15 : The amount of energy lost by evaporation according y at different position (x = 0.00 mm, z = 0.00 mm),(x = 0.25 mm, z = 0.00 mm),(x = 0.50 mm, z=0.00 mm)at t=0.33 ms. 40

Figure III.16 : : Energy lost by convection, radiation and evaporation in the weld center as a function of time. 41

Figure III.17 : Total energy lost by radiation, convection and evaporation as a function of time. 41

Figure III.18 : The ratio between energy lost by radiation, convection, evaporation and the energy of laser beam according time in the plate. 42

List of tables

Chapter II

Table II.1: Thermophysical properties of solid, liquid, solid/liquid phases. 25
Table II.2: Physical properties used in the calculations. 25
Table II.3: Variation of thermal conductivity with temperature. 25
Table II.4: Variation of density with temperature. 26
Table II.5: Variation of thermal conductivity with temperature. 26

Chapter III

Table III.1: The amount of energy lost by convection and radiation according time. 38

General introduction

General introduction

Lightweight alloys have been adopted in automotive and aerospace industries. Magnesium-based alloys are among the promising materials. Due to their good mechanical properties, they have been used also for numerous non-automotive interesting applications like in communication and engineering. Many aspects and various applications of welding are illustrated in work of C.N. Shravan et al. [1] .

Laser welding presents a many advantages owing to its high heat input [2] which lead to small heat-affected zones (HAZ).That why it's important to develop numerical simulation in order to simulate the thermal consequences of laser welding because experience can be difficult, time-consuming, and expensive

Several works have focused on numerical analyses of welding in order to explain the physics of some phenomena that occur during welding. Thus, numerical modeling is a powerful tool for understanding welding conditions and parameters. Abderrazak et al. [3] used numerical model to analyze the formation of pools of molten metal during laser welding without considering energy losses. S. Bannour et al. [4] have studied the temperature dependence of physical properties during welding. Several authors have shown that energy dissipates on surface by convection and radiation, A. Belhadj et al. [5] considered surface convection losses; they assumed the losses by radiation are on surfaces irradiated with the laser beams. They develop a model for simulating thermal history during laser welding. Abderrazak et al. [6] develop a thermal model for predicting the different parameters expected during the welding of magnesium alloys. A.K. Unni et al. [7] developed a modeling of heat transfer and heat flow during keyhole laser welding of stainless steel.

In laboratory of radiation and plasma and physics of surface (LRPPS) at Kasdi Merbah Ouargla University, several works concerning welding simulation has done since 2008 [8-14].

The purpose of our work is to calculate the distribution of temperature of magnesium alloy during laser welding. This work contains three chapters as follows:

In the **first chapter** we present generalities (definitions and physical parameters) of laser and laser welding, meaning and principle, also types of laser used for welding, we also present the principle equations for this phenomenon.

In the **second chapter**, we mention the physical phenomena of laser welding of metallic alloy (AZ91) . We choice the heat equation for liquid and solid phases and the flow equation for phase change. To resolve the problem, we present most important steps of the mathematical and numerical processing.

The **third chapter** is a presentation of the results of the calculation using numerical calculation program in Fortran77 language. Results of the calculation are discussed.

Finally we will finish by **general conclusion and perspectives**.

References

[1] C. Shravan, N. Radhika, N.H. Deepak Kumar, B. Sivasailam : A review on welding techniques : properties, charaterisations and engineering applications, Advances in Materials and Processing Technologies, (2023).

[2] S.T. Auwal, S. Ramesh, F. Yusof, S.M. Manladan,.: A review on laser beam welding of titanium alloys. Int. J. Adv. Manuf. Technol. (2018).

[3] K . Abderrazak, S. Bannour, H. Mhiri, G. Lepalec, M. Autric.: Numerical and experimental study of molten pool formation during continuous laser welding of AZ91 magnesium alloy. Comput. Mater. Sci. 44, 858–866 (2009).

[4] S. Bannour, K. Abderrazak, H. Mhiri,G. Le Palec : Effects of temperature-dependent material properties and shielding gas on molten pool formation during continuous laser welding of AZ91 magnesium alloy. Opt. Laser Technol. 44, 2459–2468 (2012).

[5] A. Belhadj, J. Bessrour, J.E. Masse, M. Bouhafs, L. Barrallier : Finite element simulation of magnesium alloys laser beam welding. J. Mater. Process. Technol. 210, 1131–1137 (2010).

[6] K. Abderrazak,W. Ben Salem, H. Mhiri,G. Lepalec, M. Autric : Modelling of CO2 laser welding of magnesium alloys. Opt. Laser Technol. 40, 581–588 (2008).

[7] A.K. Unni, V. Muthukumanan : Modeling of heat transfer, fluid flow, and weld pool dynamics during keyhole laser welding of 316 LN stailess steel using hybrid conical-cylindrical heat source, The International Journal of Advanced Manufacturing Technology, 122:3623-3645, (2022).

[8] H. Daoui : Contribution à l'étude du comportement fluide de plasma lors de l'interaction des torches à plasma avec les métaux, Academic master, University of Ouargla, (2008).

[9] K. Telib : Étude de la soudure au laser aux limites des températures de fusion des métaux, Academic master, University of Ouargla, (2013).

[10] S. Khemgani : Étude du rayonnement thermique lors de la soudure au Laser de plaques métalliques, Academic master, University of Ouargla, (2014).

[11] F. Hathat :Étude des vitesses de gaz de protection dans les dispositifs de soudage aux lasers de pièces d'alliages métalliques, Academic master, University of Ouargla, (2017).

[12] S. Benchaa : Répartition spatiale et temporelle d'énergie de sources lasers utilisées dans les dispositifs de soudage aux lasers de pièces d'alliages métalliques, Academic master, University of Ouargla, (2017).

[13] S. Lemkeddem, F. Khelfaoui, O. Babahani : Calculation of energy lost by radiation and convection during laser welding of TA6V titanium alloy, Journal of Theoretical and Applied Physics, 12(2), 113-120, (2018).

[14] S. Guerrida, F. Kelfaoui, S. Lemkeddem, K. Thlib, Z. Ballah: Calculation of spatial and temporal distribution of temperature and velocity of a weld pool during laser welding, Welding International, (2022).

Chapter I

Overview of Laser Welding and Heat Sources

Chapter I:

Overviewof Laser Welding and Heat Sources

1. Welding

Welding is a permanent joining process in which two pieces of metal are joined together to form one piece by heating the metals to their melting points. Additional metal, also called filler metal may be added during the heating process to help bind the two pieces together.

In general, it is a process in which two similar or dissimilar metal pieces can be joined by heating them to a temperature high enough to fuse the metals with or without the application of pressure and with or without the aid of filler.

2. Generalities about laser

The word "LASER" is an acronym for "Light Amplification by Stimulated Emission of Radiation". A laser is a device that produces a coherent and focused beam of light through a process called laser generation.

2.1.Components of a laser

A laser consists of several key elements:

- **Laser medium**: The laser medium is the material where the laser is generated. In the case of solid state lasers, the laser medium is formed by using a host material doped with the active laser element. The choosing operation for a laser medium is based on the laser application and the desired properties. For instance different types of host material can be used such as ruby, Nd:YAG, and doped optical fibers these materials vary in terms of the produced laser power, frequency range, and flexibility in shaping.
- **Pump source:** The pump source provides the necessary energy to the laser medium, exciting the atoms or molecules within the medium and enabling laser generation.
- **Laser resonator:** The laser resonator controls how the laser is generated within the laser medium. It consists of a rear 100 percent reflector and a front partial reflector. The resonator helps maintain the optical feedback required for the laser to oscillate and produce a coherent beam. **Figure I.1** illustrates fundamental elements of a laser system.

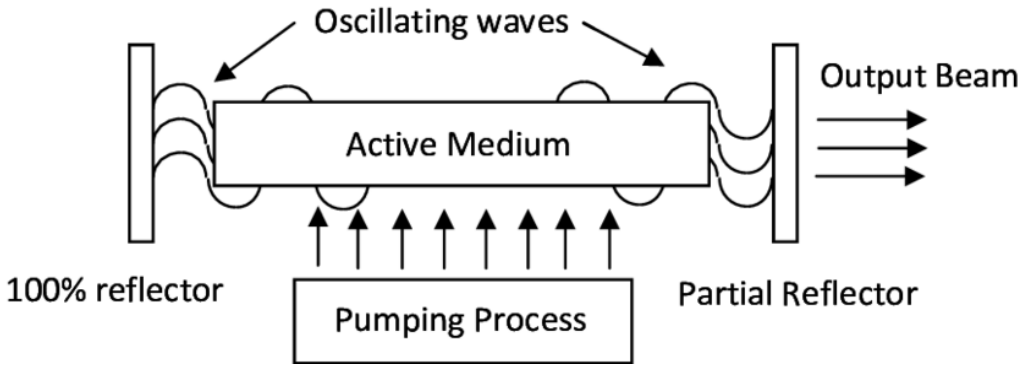

Figure I.1: Diagram illustrating fundamental elements of a laser system [1].

2.2. Principle of laser generation

Radiation interacts with atoms or particles of matter through some phenomena that occur during this process:

- **Spontaneous emission**: The pump source supplies energy to the laser medium, causing the atoms or molecules within the medium to become excited. This excitation raises the electrons to higher energy levels temporarily. However, the electrons cannot remain in this excited state indefinitely and eventually drop down to lower energy levels, releasing photons in the process.
- **Stimulated emission:** When a photon passing by an excited electron interacts with it, the electron can be stimulated to emit an additional photon that is in phase and has the same energy and direction as the incident photon. This process of stimulated emission amplifies the initial photon, resulting in the emission of more photons with the same properties.
- **Absorption:** is the process which the optical energy is converted to the internal energy of electrons, atoms, or molecules. When a photon is absorbed, the energy may cause an electron in an atom to jump from a lower energy level to a higher energy level.
- **Optical feedback:** The emitted photons travel back and forth between the mirrors of the laser resonator, reflecting and amplifying each time they pass through the laser medium. This constructive interference builds up the intensity of the light, leading to the formation of a coherent laser beam that exits through the partially reflecting front mirror.

Figure I.2 illustrates the forms of interaction between radiation and matter.

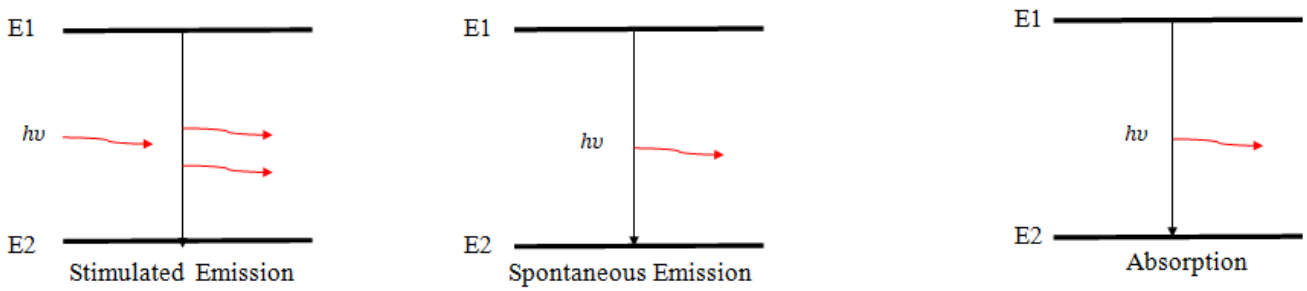

Figure I.2: Modes of radiation interaction with matter.

3. Laser welding

Laser Beam Welding (LBW), as the name suggests, is used as a concentrated source of metal melting and seam creation. LBW's high energy density leads to small areas affected by heat. The laser beam size typically ranges from 0.2 to 13 mm, making it suitable for welding materials of varying thickness and producing better result compared to the traditional welding process.

Laser welding quickly creates high -quality seams under careful tolerance. This process is generally automated and used by car and medical and jewelry industries.

3.1.Laser welding mechanisms

Laser welding can be carried out by one of two mechanisms:

- **Conduction limited welding;** where the laser acts like a point source of energy moving across the surface of the sheet. Welds formed by this process are roughly semi-circular in cross section.
- **Keyhole welding;** where the laser acts as a line source of energy penetrating into the body of the material. This line source travels across the sheet producing welds which are narrow and deep [1].

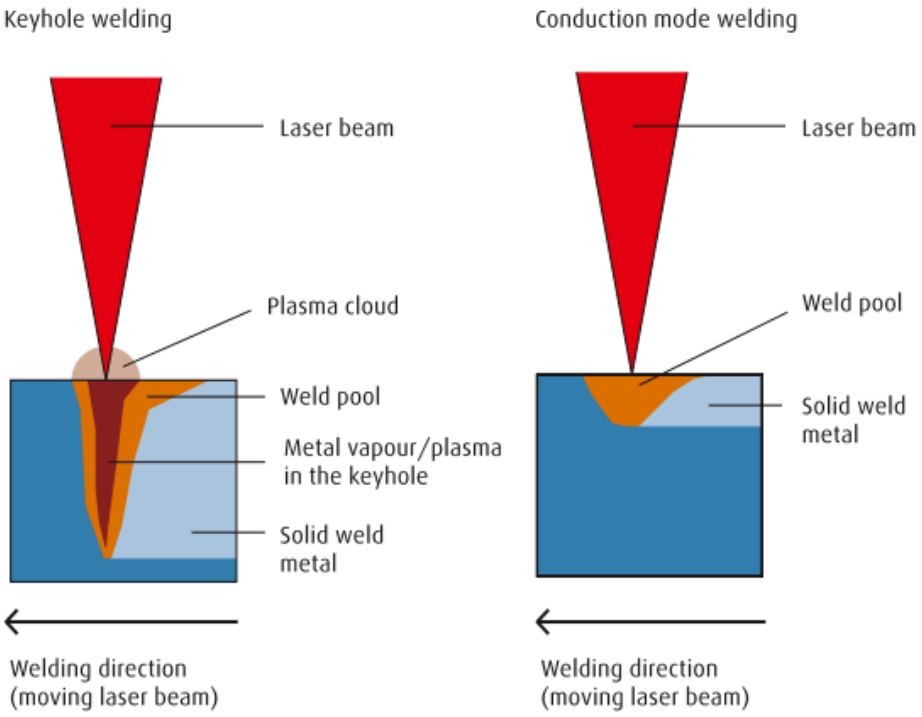

Figure I.3: Conduction mode welding and Keyhole mode[3] **.**

The principle of conduction limited welding is simple. The laser beam irradiates the material surface and heat is conducted radially away from thelaser-material interaction zone. The molten pool thus established has asemi-circular type cross section as shown in figure 4. The depth-to-width ratio of welds of this sort gives them a higher tolerance to poor fit up than keyhole type welds. As a joining process however, conduction limited welding is far less efficient than keyhole welding in terms of energy consumed per unit area of join.

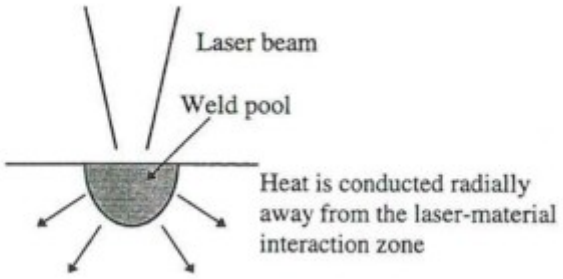

Figure I.4: Conduction limited welding [4].

4. Deep penetration keyhole welding

When deep penetration welds are produced the laser acts as a line source of energy throughout the depth of the material rather than a point source acting from the top surface only. This line source welding mechanism is made possible by the generation of a keyhole that penetrates into the material. The keyhole takes the form of a narrow, deep cavity filled vapor surrounded by molten metal. As the laser beam is moved across the metal sheet, the liquid metal flows, the keyhole solidifies behind it. The formation of the keyhole occurs only at high power densities ($\geq 10^6$ W cm^2). **Figure I.5** illustrates the keyhole and the melt pool.

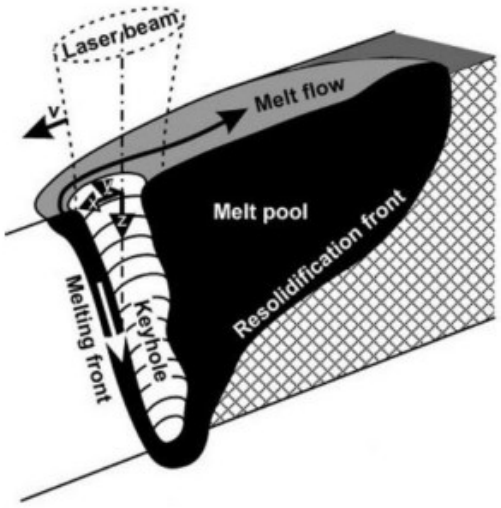

Figure I.5: Sketch of laser beam, keyhole and melt pool[5].

5. Laser Welding types

Depending on the nature of the excited medium, lasers are classified into five types: solid laser, gas laser, semiconductor laser, liquid laser and free electron laser.For a laser to be suitable for industrial applications in material processing, we require that it have a reasonable power efficiency and can be increased to the power level required to do the intended application, very few lasers fully meet these obvious requirements.

1) **Carbon dioxide laser:**

   A gaseous laser that radiates at a wavelength of 10.6 micrometers. With an efficiency of up to 15%, it is the only laser manufactured for continuous power levels of 10 kW and beyond. Although there is currently the largest number of industrial carbon dioxide synthesized. The resulting laser beams operate with a power of less than 3 kilowatts [2][3].

2) The Nd:YAG laser:

Its operating wavelength is 1.06 micrometers. Most lasers of this type have an average power of several hundred watts, maximum power pulses 1-10 kilowatts (although 1000 kilowatts can be used). This laser has a continuous power of up to 3 kilowatts.

This laser is now commercially available, and metals also have higher surface absorption at this lower wavelength. Its total efficiency ranges from 3% to 5%, unlike carbon dioxide lasers.

The beam can be directed through flexible glass fibers, because of its smaller wavelength. This makes it attractive for 3D processes that, coupled with customized arm robots, provide greater flexibility, accessibility and lower cost compared to CO_2 lasers for using a complex mirror system.

Optical lenses and fiber optics also provide a source of well-defined size and an angular radiating cone, with an even energy distribution at the top of the hat, in contrast to the fuzzy energy distribution associated with a CO_2 laser source coupled to a replica-based delivery system. There is a wide use of Nd:Yag in the electronics industry[2][3][4][5].

3) Excimer gas laser:

These compounds work in the ultraviolet region (examples: 248 nm and 193 nm). They have an efficiency of 2-4%. It produces short pulses (tens of nanoseconds) and very high peak powers (over 107 watts). The life of the optical elements is low. It usually emits roughly rectangular beams with an aspect ratio of 2/3, and low beam quality ($K<0.01$) in both directions. It is not easy to focus the beam on a small spot. These lasers have been used in lithography [2].

4) Diode lasers:

These lasers operate at a wavelength in the near-infrared region of the spectrum (such as 808 nm), which is an advantage of these lasers when compared to CO_2 and Nd:Yag, as with many lasers it has an efficiency of up to 50%. To produce high energy beams it is necessary to modulate and combine the radiation from a large number of diode emitting objects. This necessitated the development of suitable optical systems, including the currently available diode lasers with the following power in the kilowatt range (up to 2.5 kilowatts), but the beam quality is lower compared to CO_2 and Nd:Yag lasers. Still, further improvements in power and beam quality are required to improve their deep penetration welding ability. However, the high power diode laser is very compact. A multi-k laser head is only the size of a shoebox. This low weight and small size of diode lasers gives them a significant advantage

over conventional carbon dioxide and carbon dioxide lasers. Nd:Yag can be directly attached to robots and moved easily. They also have lower cooling requirements and a longer lifespan (for all diodes: 5,000-10,000 hours). The size of this system is limited mainly by the amount of cooling required and will not be affected much by further improvements in semiconductor technology [6][2][7].

6. Welding Factors

Every laser manufacturing technique is accompanied by a set of variables that impact the quality of welding process. There are many types of parameters, where the Ishikawa line is a useful tool for structuring and analyzing a complex production process according to its parameters. The factors affecting the laser can be summarized under the following elements:

1. Laser source
2. Parent materials
3. Beam parameter
4. Jigs, fixture and tooling
5. Mechanical parameters
6. Joint design
7. Shielding gas
8. Beam positioning (welding position, beam incident angle, defocusing etc.)

These weld characteristics in turn determine the mechanical properties of the welded joints. The selection of the welding process parameters is therefore essential for obtaining the welded joint ensuring desired weld-bead geometry, excellent mechanical properties with minimum distortion

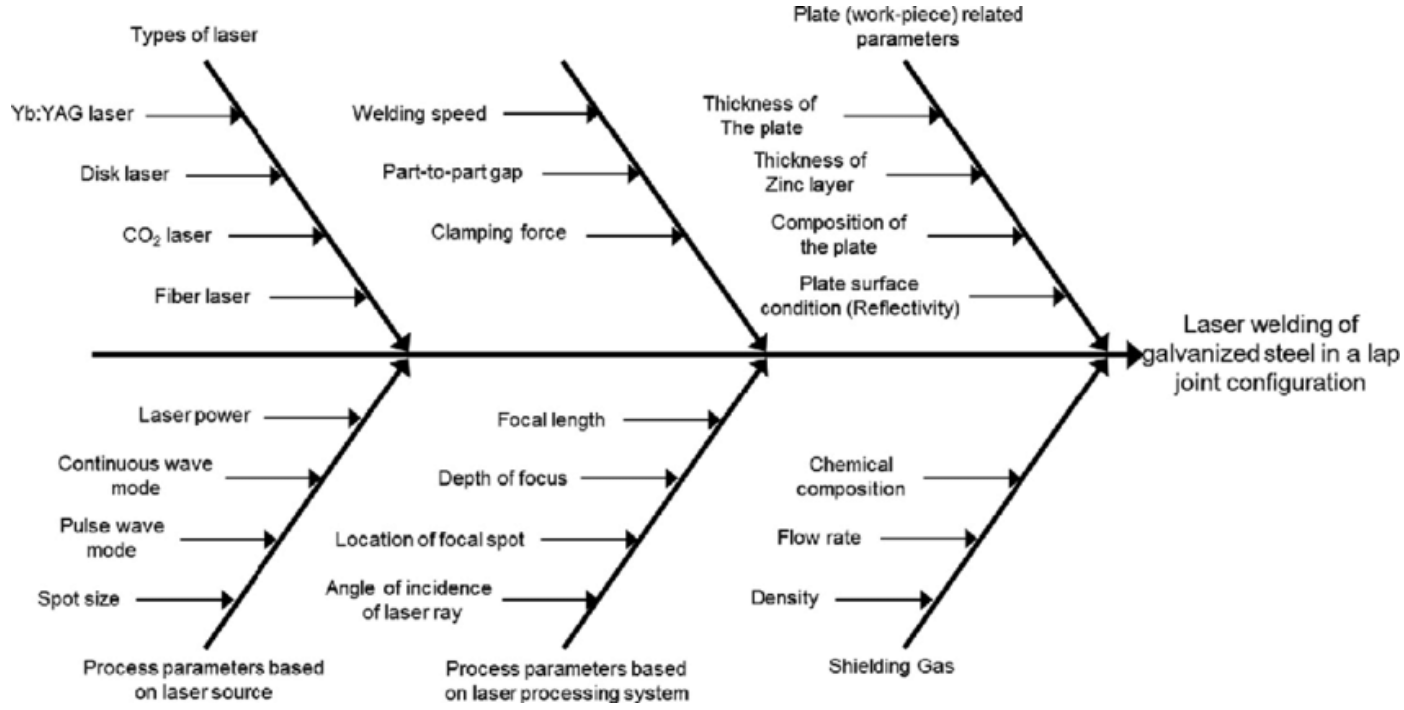

Figure I.6: Ishikawa diagram showing the factors affecting the laser weld quality[13].

7. Conservation equations

- **Conservation mass equation:**

The Conservation of mass equation of a compressible or incompressible fluid takes the following form [10]:

$$\frac{\partial \rho}{\partial t} + div\left(\rho \vec{V}\right) = 0 \qquad \textbf{(I.1)}$$

- **Conservation of momentum equation:**

The momentum conservation equation or Navier's equation Stocks takes the following form [11]:

$$\frac{\partial \rho \vec{V}}{\partial t} + div\left(\rho \vec{V}\vec{V}\right) = 0 \qquad \textbf{(I.2)}$$

- **Energy Conservation equation:**

The equation of the energy of an incompressible fluid is the following:

$$\rho . c_p . \frac{\partial T_{(x,y,z,t)}}{\partial t} = k \nabla^2 T_{(x,y,z,t)} + Q(i,j,k) \quad \textbf{(I.3)}$$

This equation is valid for both solid and liquid state processing. In the case of phase change we apply another equation, the calculation of the total energy flow is with the following expression [11]:

$$d\varphi = (-\lambda \overrightarrow{grad T} . \overrightarrow{dS} + Q(i,j,k) . dV) . dt \quad \textbf{(I.4)}$$

C_p: Specific heat (J/kg K).

P: Volume density (kg/m³).

λ: Thermal conductivity (W/m K).

dφ: Heat flux (J).

Q: The source term (W/m³).

dV: The elementary volume (m³).

dt: The time step(s).

8. Energies loss in laser welding

During laser welding, the material's surface undergoes heating, resulting in the melting or fusion of a portion of it. This fusion is accompanied by the dissipation of energy, as heat is transferred to the metal sheets through radiation, thermal conduction, and metal evaporation.

This study is an extension of a previous study conducted by S. Lemkeddem et al. [18], where the aspect of energy loss through vaporization was neglected, and the amount of energy lost through thermal conduction and radiation during laser welding of thin sheets of titanium alloys (TA6V) was determined. It is also an extension of previous work on studying material loss through vaporization in laser welding or cutting processes of metals [19].

- The loss of energy by Thermal convection at level of the plates during and after welding is given by [20] [21]:

$$Q_{conv} = h(T - T_0) \quad \textbf{(I.5)}$$

h : Heat transfer coefficient (W/m^{2}K)

T and T_0: are Current Temperature and Room temperature respectively.

- The energy loss through radiation is given by the following expression [20] [21] [22]:

$$Q_{ray} = \sigma\varepsilon\left(T^4 - {T_0}^4\right) \quad \textbf{(I.6)}$$

σ : Constant of Stefan-Boltzmann (W/m^2 K^4)

ε : Permittivity of free space.

When the materials are exposed to the laser beam this leads to the evaporation of part of the material which means that there is a loss in energy, and the energy is dispersed due the vapor with the surrounding particles. The expression of energy loss by evaporation is given by[23]:

$$Q_{vap} = \rho\vartheta_{ev}L_{ev}\pi R^2 \quad \textbf{(I.7)}$$

ρ: Volemetric density in the liquid phase (kg/m^3)

ϑ_{ev}: Evaporation speed (m/s)

L_{ev}: Latent heat of evaporation (J/kg)

R: laser radius (m)

The energy loss through evaporation can be expressed by the following equation [24]:

$$Q_{vap} = \rho_m L_v V_v \quad \textbf{(I.8)}$$

V.Semak et al. used the term V_v as follows:

$$V_v = V_0 \exp\left(-\mu/T_s\right) \quad \textbf{(I.9)}$$

$$\mu = ML_v/K_B N_a \quad \textbf{(I.10)}$$

$V_0$was expressed by the following expression:

$$V_0 = \sqrt{5RT_s/3M} \quad \textbf{(I.11)}$$

Reducing energy loss through vaporization and increasing the efficiency of the welding process depend on various factors such as laser power and focus, material properties, and process conditions. Improving laser design, settings, and material selection can help minimize energy loss and enhance the efficiency of laser welding.

9. Influence of shielding gases in the welding process

Shielding gases are of considerable importance in protecting weld metal from atmospheric contamination during welding processes. These gases play an important role in a number of aspects of welding, including the characteristics of the weld and the microstructure of the welded parts. It is therefore important to understand the influence of welding shielding gases on different materials, and many researchers have carried out extensive studies and experiments. Shielding gases in laser welding processes have a remarkable effect on the overall performance of the welding system. The main function of these gases is to protect the weld pool from undesirable reactions to atmospheric

gases. Oxygen, nitrogen and water vapor in the ambient air can cause weld contamination. The shielding of welds therefore always involves the removal of potentially reactive gases from the vicinity of the weld, thus preventing the adverse effects of the surrounding atmosphere on the molten metal.

Shielding gas also interacts with the base metal and filler metal and can thus change the basic mechanical properties of the welded area, such as strength, toughness, hardness and corrosion resistance. Additionally have significant effects on weld bead formation and penetration pattern. Application of different protective pads may result in different penetration and weld bead profiles. Weld porosity is one of the most common welding defects related to the protective atmosphere. Pots can be the point of initiation of crack propagation in the welded joint and can significantly decrease the life cycle of joints subjected to dynamic loads [8][9].

11. References

[1] A. Mudassar;**"**A few glimpses from the book of Laser physics**"**, first edition, page 3,(August 2015).

[2] A. Kaplan**;"**Modellrechnung und numerische Simulation von Absorption**"**;Wärmeleitung und Strömung des Laser-Tiefschweißens Dis-sertation der TechnischenUniversität Wien, Austria, (1994).

[3] LASERLINE Technical Laser Welding**;"** Two different methods of laser welding**"**, edition 402935, page 4,(17 August 2009).

[4] C. Lampa;**"**Laser Welding-Energy Redistribution and Weld Geometry**"**, Doctoral Thesis, Lulea University of Technology, 1997:33, ISSN: 1402-1544, page 5.

[5] A. Kaplan;"Fresnel absorption of 1μm- and 10μm-laser beams at the keyhole wall during laser beam welding: Comparison between smooth and wavy surfaces**"**;Applied Surface Science,**258**(8), 3354-3363(2012).

[6] L.H.J.F. Beckmann, D. Ehrlichmann;"Optical systems for high-power laser applications: principles and design aspects"; Optical and Quantum Electronics, **27**, 1407-1425(1995).

[7] J. Rapp, C. Glumann, F. Dausinger, H. Hügel ;**"**Optical and Quantum Electronics**"**,**27**, 1203-1211(1995).

[8] N. Blundell, J. Biffin, T. Johnson, C.Page;**"**Trends in Welding Research: Proceedings of the 5th International Conference (1998)**"**, Ed. J.M. Vitek, S.A. David, J.A. Johnson, HB. Smartt, T. DebRoy. Printed 1999 by ASM International,483-487(1999).

[9] Y. Tzeng;"Parametric analysis of the pulsed Nd:YAG laser seam-welding process"; J. Mat. Proc. Tech, **102**, 40-47(2000).

[10] E. Schubert, M. Grupp, G. Sepold;"MaterialbearbeitungmitHochleistungsdioden-lasern."(Teil1); Laser Magazin,**2**,14-17(1998).

[11] H.J.F. Beckmann, D. Ehrlichmann;**"**Optical Systems for high-power laser applications: principles and desin aspects**"**;Optical and Quantum Electronics**, 27**, 1407-1425, (1995).

[12] F. Bachmann. Rofiin-Sinar Laser GmbH, 18.11.98.

[13] A.K. Sinha, D.Y. Kim, D. Ceglarek;"Correlation Analysis of the Variation of Weld Seam and Tensile Strength in Laser Welding of Galvanized Steel";Optics and Lasers in Engineering, **51**(10),1143-1152(2013).
https:// doi.org/10.1016/j.optlaseng.2013.04.012

[14] ASM International. Handbook Committee. Knovel (Firm) (1993) ASM handbook,Volume 6: Welding, Brazing, and Soldering.

[15] J. M. Kuk, K.C. Jang, D.G. Lee, I.S. Kim;**"**Effects of temperature and shielding gas mixture on fatigue life of 5083 aluminum alloy**"**; Journal of Materials Processing Technology, **155**, 1408-1414(2004).

[16] J. Roǹda, A. Siwek;"Modelling of laser welding process in the phase of keyhole formation"; University of Science and Technology, Poland, Archives of civil anmechanicalengineering, (3), 742 (2011).

[17] B. Morgan;**"**Mécanique des fluides**"**; Résumé de Cours, Ecole Normale Supérieurede Cachan, (2009).

[18] S. Lemkeddem, F. Khelfaoui, O. Babahani;"Calculation of energy lost by radiation and convection during laser welding of TA6V titanium alloy";J.Theor. Appl. Phys., **12**(2), 113(2018).
Doi: 10.1007/s40094-018-0288-x

[19] مروة حجاج و بن الشرع كلثوم، دراسة ضياع المادة عن طريق التبخرحالةلحام أو قطع المعادن بواسطة الليزر، مذكرة ماستر أكاديمي،جامعة ورقلة(2020).

[20] R. Rai, J.W. Elmer, T.A. Palmer, T. DebRoy;"Heat transfer and fluid flow during keyhole mode laser welding of tantalum"; Ti–6Al–4V, 304L stainless steel and vanadium, J. Phys. DAppl. Phys. **40**, 5753-

5766(2007).
https://doi.org/10.1088/0022-3727/40/18/037

[21] E. d. S. Magalhaes, A. L. F. de Lima e Silva, S. M. M. de Lima e Silva;**"** A GTA Welding Cooling Rate Analysis on Stainless Steel and Aluminum Using Inverse Problems**"**;Applied Sciences,**7**(2), 122-137(2017).
https://doi.org/10.3390/app7020122

[22] H.G. Fan, H.L. Tsai, S.J. Na;**"**Heat transfer and fluid flow in a partially or fully penetrated weld pool in gas tungsten arc welding**"**; Int. J. Heat Mass Transf., **44**, 417-428(2001).

[23] M. Mostafa;"Etude du perçage et du soudage laser: dynamique du capillaire"; Doctoral Thesis, Université de Bourgogne, (2011).

[24] V. Semak, A. Matsunawa;"The role of recoil pressure in energy balance during laser materials processing"; J. Phys. D. Appl. Phys., **30**(18), 2541(1997).

Chapter II:
Numerical modeling of heat equation

Chapter II: Numerical modeling

1. Introduction

In this chapter, we will present the numerical modeling used to calculate the temperature in three dimensions. We use the Finite Difference Method (FDM). The calculation is based on solving the differential equation of heat diffusion; we descretize the field of study by developing Taylor series derivatives.

2. Physical phenomenon

During laser welding, on the workpiece surface several phenomena proceed. One of them is the beam absorption connected with two mechanisms: Fresnel absorption and inverse bremsstrahlung. Energy of laser beam is dissipated because of multiple reflecting of light, radiation, convection, evaporation, and energy absorption by plasma created in keyhole. The energy absorbed by a surface is related to radiation intensity, radiation length, shape and porosity of a material surface, and presence of plasma above a surface [1].

The processing of an AZ91 magnesium alloy plate, sized 5mm×5mm×2mm, was considered in this work. The laser heat source was located at point (0,0,0). The equations are written in a Cartesian coordinate system. **Figure II.1** illustrates a schematic representation of the geometry, coordinate and region on which laser beam directly acts.

We will study the temperature (energy) changes in the laser welding process for this alloy. The Configuration of laser welding and coordinates system are shown in **figure II.1**. We consider that there is energy loss by radiation, convection and evaporation. This welding is for two identical metals. The work to be done is the distribution of temperature over volume as a function of time in welding plates using a stationary laser.

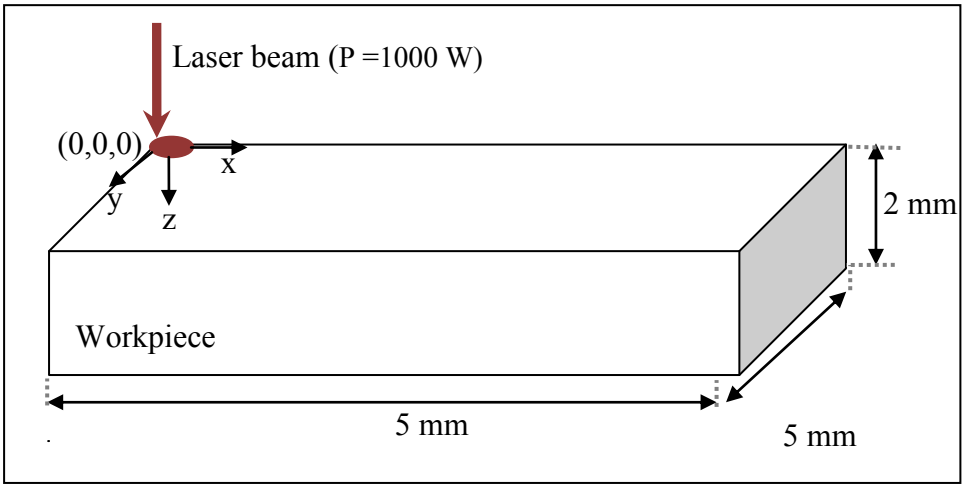

Figure II.1: Configuration of laser welding and coordinates system.

3. Hypotheses

In this work, we considered the following hypotheses:

- Three dimensions problem.
- A non-moving laser with a size distribution of the source term.
- Presence of losses (by convection, radiation, evaporation).
- Physical properties (heat capacity or specific heat, thermal conductivity) are variable with the change of temperature.

4. Mathematical Model

To find the distribution of heat in the volume of the material it is necessary to take account the nature of the phase.

The principal equation, that is necessary to calculate distribution of temperature for solid phase (s) and the liquid phase (l), is the heat equation [2]:

$$\left[\frac{\partial \rho\,(T) Cp(T) T(x,y,z,t)}{\partial t}\right] = div\,(\lambda(t)\,\overrightarrow{grad}\,T\,(x,y,z,t) + Q(x,y,z) + \frac{Q_{losses}}{dVdt} \qquad \textbf{(II.1)}$$

With :

$$Q_{losses} = Q_{rad} + Q_{conv} + Q_{evap}$$

$$Q_{evap} = (\rho V_v L_{ev} \pi R^2)/dV$$

$$Q_{rad} = \sigma\varepsilon\,(T^4 - {T_0}^4)$$

$$Q_{conv} = h\,(T - T_0)$$

Where:

Q_{rad} : Energy lost by radiation (J)

Q_{conv} : Energy lost by convection (J)

Q_{evap} : Energy lost by evaporation (J)

For the solid-liquid phase change, we use the heat flux equation [3]:

$$d\varphi = Q(x,y,z)\, dV\, dt \tag{II.2}$$

5. Numerical model

For numerical model, the Finite Difference method (FDM) was used. This method depends on the approximation of partial derivation of Taylor's expansions of function T(x,y,z,t).

5.1. Taylor development:

Taylor's expansions of function T(x,y,z,t) according to x,y,z are:

$f(x+hx, y+hy, z+hz)$

$$= f(x,y,z) + hf'(x,y,z) + \frac{h^2}{2!}f^{(2)}(x,y,z) + \cdots + \frac{h^n}{n!}f^{(n)}(x,y,z) \tag{II.3}$$

$f(x-hx, y-hy, z-hz)$

$$= f(x,y,z) - hf'(x,y,z) - \frac{h^2}{2!}f^{(2)}(x,y,z) - \cdots - \frac{h^n}{n!}f^{(n)}(x,y,z) \tag{II.4}$$

Partial derivative approximation of time:

$$\frac{\partial T}{\partial t} = \frac{T^n{}_{(i,j,k)} - T^{n-1}{}_{(i,j,k)}}{dt} \tag{II.5}$$

Partial derivative approximation of tow ranks:

$$\frac{\partial^2 T}{\partial x^2} = \frac{T^n{}_{i-1,j,k} - 2T^n{}_{i,j,k} + T^n{}_{i+1,j,k}}{dx^2} \tag{II.7}$$

$$\frac{\partial^2 T}{\partial y^2} = \frac{T^n{}_{i,j-1,k} - 2T^n{}_{i,j,k} + T^n{}_{i,j+1,k}}{dy^2} \tag{II.8}$$

$$\frac{\partial^2 T}{\partial z^2} = \frac{T^n{}_{i,j,k-1} - 2T^n{}_{i,j,k} + T^n{}_{i,j,k+1}}{dz^2} \quad \textbf{(II.9)}$$

Where dt is the time step for an index n, dx, dy and dz are the following discretizationsteps the coordinates x, y and z with the indices i, j and k respectively.

The finite difference method was applied to points of grid by applying partial derivatives in the heat and heat flow equations, until we reach the following equations:

- **For the solid and liquid phases:**

$$Cp^n(T)\rho^n(T)\left[\frac{T^n(i,j,k) - T^{n-1}(i,j,k)}{dt}\right] = \lambda^n(T)\left\{\begin{array}{l}\dfrac{T^n(i-1,j,k) - 2T^n(i,j,k) + T^n(i+1,j,k)}{dx^2} \\ + \dfrac{T^n(i,j-1,k) - 2T^n(i,j,k) + T^n(i,j+1,k)}{dy^2} \\ + \dfrac{T^n(i,j,k-1) - 2T^n(i,j,k) + T^n(i,j,k+1)}{dz^2}\end{array}\right\} + Q(i,j,k) + Q_{losses} \quad \textbf{(II.10)}$$

We get the following equation:

$$-\alpha_3 T^n{}_{i,j,k-1} + \big(1 + 2\,(\alpha_1 + \alpha_2 + \alpha_3)\big)T^n{}_{i,j,k} - \alpha_3 T^n{}_{i,j,k+1} = B_s(k) \quad \textbf{(II.11)}$$

Where the parametersα_1 , $\alpha_2, \alpha_3, \alpha_4, \mathrm{B_s(k)}$ are:

$$\alpha_1 = \frac{\lambda^n(T)dt}{Cp^n(T)\rho^n(T)dx^2}$$

$$\alpha_2 = \frac{\lambda^n(T)\,dt}{Cp^n(T)\rho^n(T)dy^2}$$

$$\alpha_3 = \frac{\lambda^n(T)\,dt}{Cp^n(T)\rho^n(T)dz^2}$$

$$\alpha_4 = \frac{dt}{Cp^n(T)\rho^n(T)}$$

$$B_s(k) = T^{n-1}(i,j,k) + \frac{\lambda^n(T)dt}{Cp^n(T)\rho^n(T)}\left\{\frac{T^n(i-1,j,k) + T^n(i+1,j,k)}{dx^2} + \frac{T^n(i,j-1,k) + T^n(i,j+1,k)}{dy^2}\right\} + \frac{dt}{Cp^n(T)\rho^n(T)}(Q(i,j,k) + Q_{losses})$$

- **For phase change:**

To account for the transition between the solid phase and liquid phase, we computed the amount of energy (the flow), dφ accumulated in an elementary volume, and we compared with the enthalpy of fusion. We assumed that the welding temperature varied linearly during the phase transition.

The temperature flow of energy in volume element of the cube mentioned in **figure II.2**

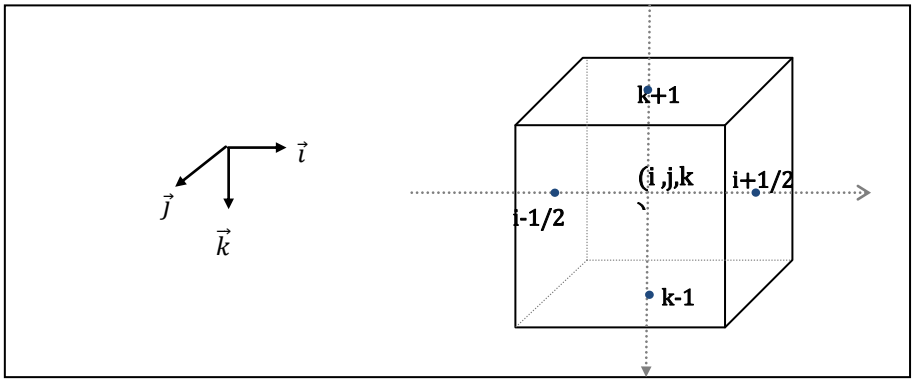

Figure II.2: Geometric model for phase change.

$$d\varphi = Q(i,j,k)\, dx\, dy\, dz\, d \qquad \textbf{(II.12)}$$

The flux must be compared with H_{min}(latent heat of fusion):

If $d\varphi < H_{min}$:

$$T_{i,j,k}{}^{n} - T_{i,j,k}{}^{n-1} = \frac{d\varphi}{H_{min}}\, \Delta T \qquad \textbf{(II.13)}$$

Else:

$$\rho\, cp\, \left(T_{i,j,k}{}^{n} - T_{f2}\right) dV = d\varphi - H_{min} \qquad \textbf{(II.14)}$$

Where:

$\Delta T = T_{f2} - T_{f1}$

ΔT : Temperature range of melting

T_f : fusion temperature.

The equations (II.11), (II.14) and (II.15) are applicable for general case: j=2, jmax-1, i=2, imax-1 and fork=2, k_{max}-1.

These equation present linear equation wich A(k_{max},k_{max})is a matrix , B(k_{max}) and X(k_{max}) are columns.

$$A(k,k-1)T_{k-1} + A(k,k)T_k + A(k,k+1)T_{k+1} = B(k) \qquad \textbf{(II.15)}$$

5.2. Initial condition and boundary conditions:

A 2D geometric model meshing is presented in **Figure II.3.**

- The initial condition is:

T (t= 0.00 s) = 300 K

- The boundary conditions are:

➢ For the farthest edge of the plate from the laser heat source (i=imax, j=jmax, k=kmax), we propose a slow variation of temperatures:

$$\left.\frac{\partial T(x,y,z,t)}{\partial x}\right|_{x=xmax} = 0 \quad \rightarrow T(imax,j,k) - T(imax-1,j,k) = 0$$

$$\left.\frac{\partial T(x,y,z,t)}{\partial y}\right|_{y=ymax} = 0 \quad \rightarrow T(i,jmax,k) - T(i,jmax-1,k) = 0$$

$$\left.\frac{\partial T(x,y,z,t)}{\partial z}\right|_{z=zmax} = 0 \quad \rightarrow T(i,j,kmax) - T(i,j,kmax-1) = 0$$

➢ For j=1 the symmetry is applied in equations **(II.10) , (II.13), (II.14)**:

With: $T(0,j,k) = T(2,j,k)$ $T(i,0,k) = T(i,2,k)$

➢ For i=1 the symmetry is applied in equation **(II.10) , (II.13), (II.14)**:

With: $T(0,j,k) = T(2,j,k)$ $T(i,0,k) = T(i,2,k)$

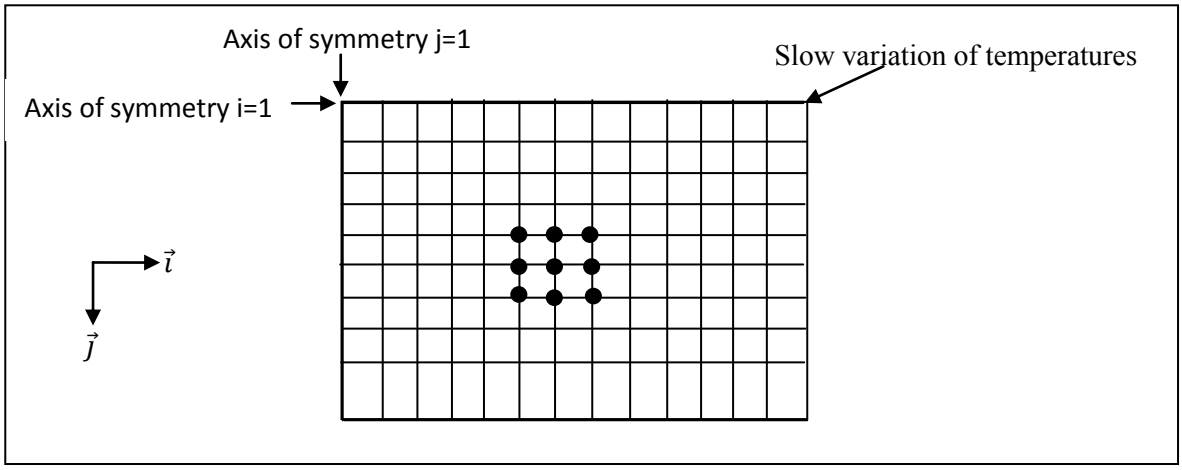

Figure II.3 :2D geometric model meshing

- For the top surface k=1 we used the midpoint k=3/2 as shown in **Figure II.4**.

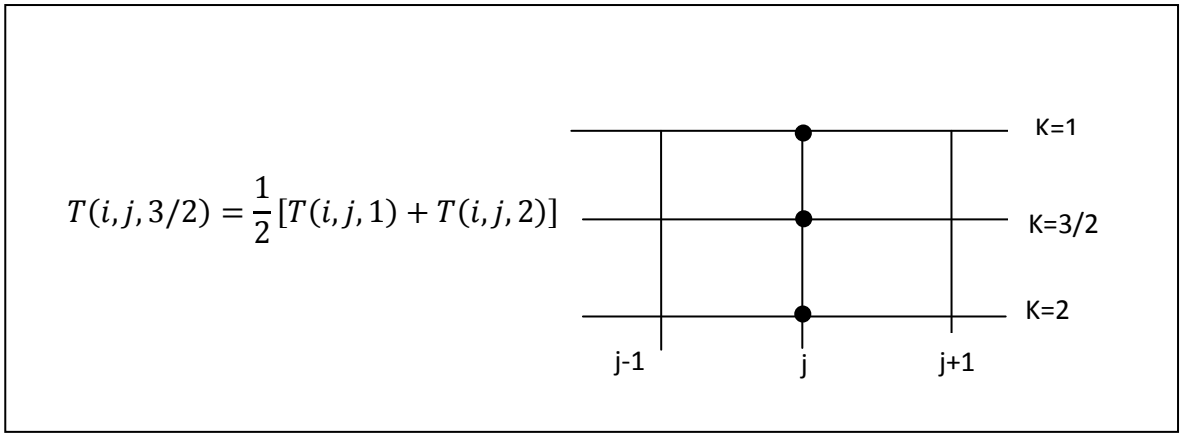

Figure II.4 : Model meshing of midpoint

For losses terms we consider that losses are related to the top surface:

$$Q_{losses}(i,j,3/2) = Q_{losses}(i,j,1)$$

5.3. Gauss–Seidel method:

We applied the Gauss–Seidel Method (GSM) which is an iterative technique for solving this square system of k_{max} coupled linear equations: A.T=B.

The matrix A is tridiagonal; T and B are vectors.

$$\begin{pmatrix} a_{11} & a_{12} & 0 & \cdots & \cdots & 0 \\ a_{21} & a_{22} & a_{23} & \cdots & \cdots & 0 \\ 0 & \ddots & \ddots & \ddots & \ddots & \vdots \\ \vdots & a_{k,k-1} & a_{k,k} & a_{k,k+1} & \ddots & \ddots \\ \vdots & \ddots & \ddots & \ddots & \ddots & \ddots \\ 0 & \ddots & \ddots & \ddots & a_{kmax,kmax-1} & a_{kmax,kmax} \end{pmatrix} \times \begin{pmatrix} T_1 \\ T_2 \\ \vdots \\ T_k \\ \vdots \\ T_{kmax} \end{pmatrix} = \begin{pmatrix} b_1 \\ b_2 \\ \vdots \\ b_k \\ \vdots \\ b_{kmax} \end{pmatrix}$$

We have:

$$T_1 = \frac{-a_{11}T_1 - a_{12}T_2 + b_1}{a_{11}}$$

$$T_k = \frac{-a_{k,k-1}T_{k-1} - a_{k,k+1}T_{k+1} + b_k}{a_{kk}}$$

$$T_{kmax} = \frac{-a_{kmax,kmax}T_{kmax} + b_{kmax}}{a_{kmax,kmax}}$$

The convergence properties of the Gauss–Seidel method are dependent on the matrix A(k_{max},k_{max}) and vector B(k_{max}).

6. Laser Heat source:

The laser heat source presents the contribution of energy in keyhole .A Gaussian laser energy distribution is commonly used to model the laser heat source; in this case the power absorbed and distributed in volume, the density of power is also distributed in volume. **Figure II.5** shows the laser heat source power density distribution.

In this study we used the heat source in the following form [4]:

$$Q(x,y,z) = \frac{3P}{abd\pi} exp\left(-\frac{3(x(i))^2}{a^2}\right) exp\left(-\frac{3(y(j))^2}{b^2}\right) exp\left(-\frac{3(z(k))^2}{c^2}\right) \quad \textbf{(II.16)}$$

Where:

a, b : Focal rays (m)

c : Maximum penetration (m)

P : Power of laser (W)

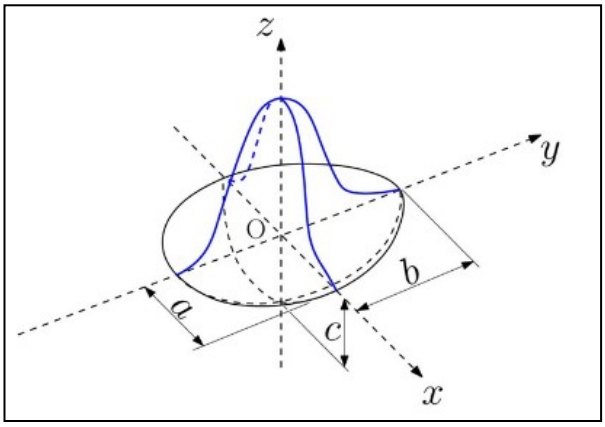

Figure II.5: Laser heat source power density distribution [5].

7. Material Properties:

Mg-AL system is one of the most widely used alloys due to his good mechanical and thermophysical properties. The plate used is AZ91 magnesium alloy (9% Al, 0.8% Zn, 0.2% Mn, 90% Mg). In this work, AZ91 melted in the range 730–750 K, the average temperature of T_f = 740 K was used as melting point. Magnesium exhibits some excellent characteristics for fusion welding. Since an important temperature gradient was produced during laser welding, the physical characteristics of the material must be temperature dependent. S. Bannour et al. [4] investigated the effect of welding temperature on the physical properties of solid and liquid AZ91.

The heat transfer coefficient, h = 5 Wm^{-2} K^{-1} [5], was temperature independent. The used absorption coefficient is ε = 0.3.

Table II.1 and **II.2** present Average values of physical properties of AZ91; we exploited these values and others in this work.

Table **II.1**: Thermophysical properties of solid, liquid, solid/liquid phases [4].

Average values	**Solid**	**Solid/Liquid**	**Liquid**
c_p (J kg^{-1} k^{-1})	1340	1180	1020
ρ(kg /m^2)	1590	1700	1810
λ(wm/k)	156	151	146

Table **II.2**: Physical properties used in the calculations [4].

Properties	**Symbol**	**Value**
absorption coefficient	ε	0.3
Boiling temperature	T_b	1380 (K)
Fusion temperature	T_f	740(K)
Vaporization temperature	T_v	870(K)
Heat transfer coefficient	h	5 (Wm^{-2} K^{-1})

7.1. Tabulation of specific heat, density and thermal conductivity for AZ91:

We considered a linear change for each of ρ, λ and C_p in function of temperature:

Table II.3: Variation of thermal conductivity with temperature [4, 6].

T**(K)**	300	350	400	500	600	800
λ**(wm/k)**	156	155	153	151	149	146

For solid phase: $\lambda(T) = 162.9569 - 0.02362\ T$
For solid/liquid phase: $\lambda(T) = 151$
For liquid phase: $\lambda(T) = 146$

Table II.4: Variation of density with temperature [4,6].

T**(k)**	273	373	473	573	923	1000	1100
ρ**(kg /m^2)**	1820	1800	1780	1760	1590	1570	1540
T**(k)**	1300	1400	1600	1800	1900	2000	
ρ**(kg /m^2)**	1490	1460	1410	1360	1330	1310	

For solid phase: $\rho(T) = 531.562 - 0.2\ T$
For solid/liquid phase: $\rho(T) = 1700$
For liquid phase: $\rho(T) = 1831.6038 - 0.263\ T$

Table II.5: Variation of thermal conductivity with temperature [4,6].

$\boldsymbol{T}$**(k)**	298.15	300	400	500	600	700	800
$\boldsymbol{C_p}$ **(J kg^{-1} k^{-1})**	605.19	605.68	631.44	655.99	680.54	704.84	729.39
$\boldsymbol{T}$**(k)**	900	923	1000	1100	1300	1600	2000
$\boldsymbol{C_p}$ **(J kg^{-1} k^{-1})**	754.18	833.66	802.06	766 .57	707.24	686.13	685.401

For solid phase: $cp(T) = 870.27 + 0.48\,T$
For solid/liquid phase: $cp(T) = 1700$
For liquid phase: $cp(T) = -2322.95 + 4.15\,T$

8. Diagram of the numerical calculation

A numerical program has been developed in FORTRAN language to calculate the temperature of AM60 alloy. The **Figure II.6** presents the diagram.

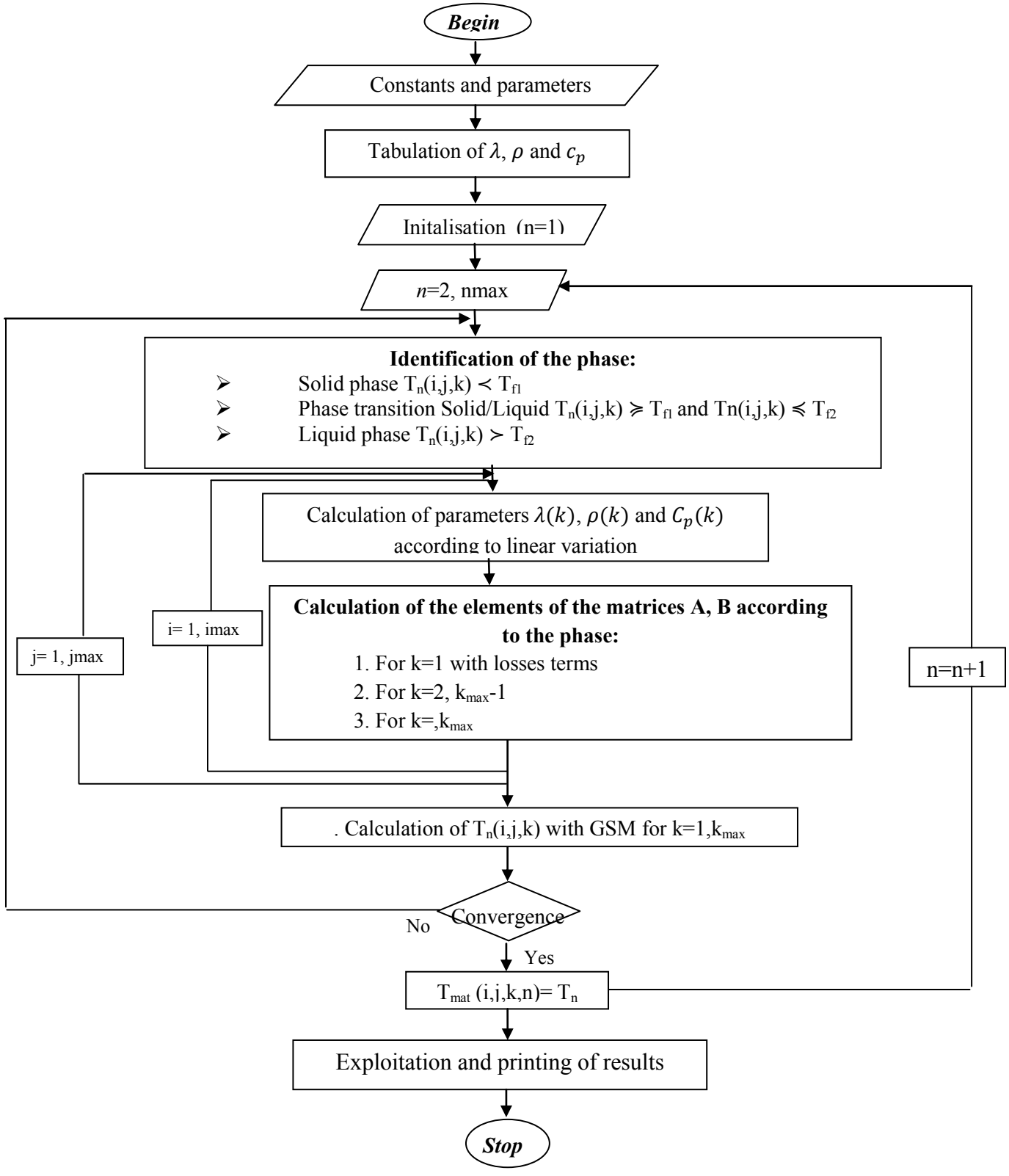

Figure II.6: Diagram to calculate the temperature

Where:

T_{mat}: Temperature of material in previous time.

T_{temp}: Save of old temperature corresponding to time (n-1).

T_n: Temperature at a given point at time n.

$[T_{f1}, T_{f2}]$: temperature range of melting

9. Conclusion

As described above, a numerical study was developed in order to investigate the impact of laser heat source on metal alloy (AZ91). To achieve this study, a Gaussian volumetric heat source was proposed to model the incident laser beam power. A FORTRAN-based computer program was used for calculation.

10.References

[1] D.T. Swit-Hook, A.E.F. Gick; ”Penetration welding with lasers”; Welding Journal, **52**, 492-299, (1973)

[2] A. Belhadj, J. Bessrour, J-E Masse, M. Bouhafs, L. Barrallier; ”Finite element simulation of magnesium alloys laser beam welding”; Journal of Materials Processing Technology, **210** (9), 1131-1137, (2010)

[3] B. Morgan; “Mécanique des fluides, Résumé de Cours“; Ecole Normale Supérieure de Cachan, (2009)

[4] S. Bannour, K. Abderrazak, H. Mhiri, G. Le Palec; ” Effects of temperature-dependent material properties and shielding gas on molten pool formation during continuous laser welding of AZ91 magnesium alloy”; Opt. Laser Technol, **44**, 2459-2468, (2012)

[5] E.J.G. Nascimento, E. Maglhas, L.E. Dos Santos Paes; ” A literature review in heat source thermal modeling applied to welding and similar processes”; The international journal of advanced manufacturing technology, **126**(7-8), 1-41, (2023)

[6] M.S. Dargusch, A. Hamasaiid, G. Dour, T. Loulou, C. J. Davidson, D. h. Stjohnl; ”The Accurate Determination of Heat Transfer Coefficient and its Evolution with Time During High Pressure DieCasting of Al-9 %Si-3 %Cu and Mg-9 %Al-1 %Zn Alloys”; Advanced Engineering Materials, **9** (11), 995-999,(2007).

Chapter III:

Results and Discussion

Chapter III: Results and Discussion

1. Introduction

Depending on numerical simulation presented in chapter II, in this chapter we resume the results and discuss them. Firstly, the heat laser source will be represented. Then we have temperatures evolution of some positions according time and axis. We will compared between different laser beam power results and between the results of temperature depended proprieties and constant properties. Finally, we will discuss the effect of losses by convection and radiation on temperature evolution and estimate the losses by evaporation.

2. Profiles of laser source

A volumetric laser source as mentioned in equation (II.17) was used where focal rays $a = b = 1\ mm$ and Maximum penetration $c = 1\ mm$.

2.1. Heat laser density according z:

Figure III.1 shows the distribution of Q according z. It's noticed that Q increase when z decrease and Q neglected in the farthest edge of the plate

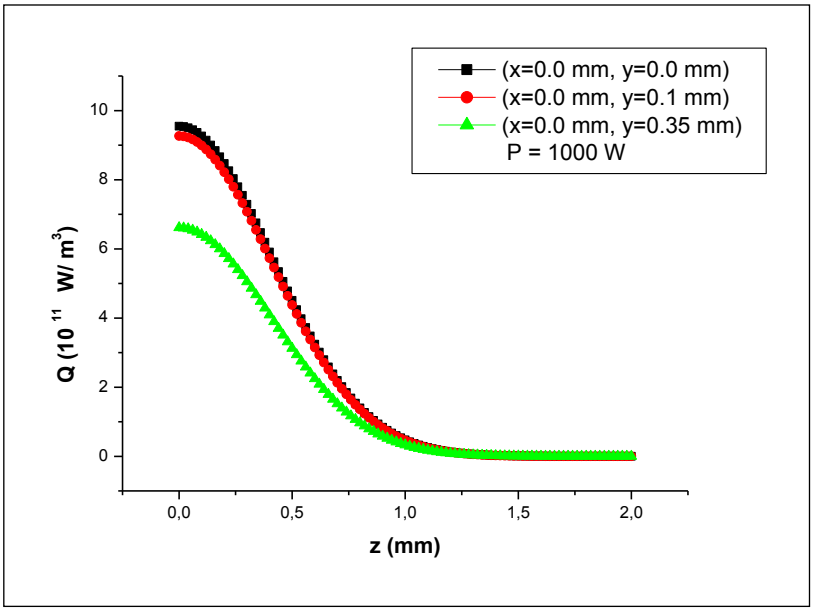

Figure III.1: Heat laser density according z.

2.1. Heat laser density according y:

Figure III.2 shows the distribution of Q according y; even here it's noticed that Q increase when x decrease.

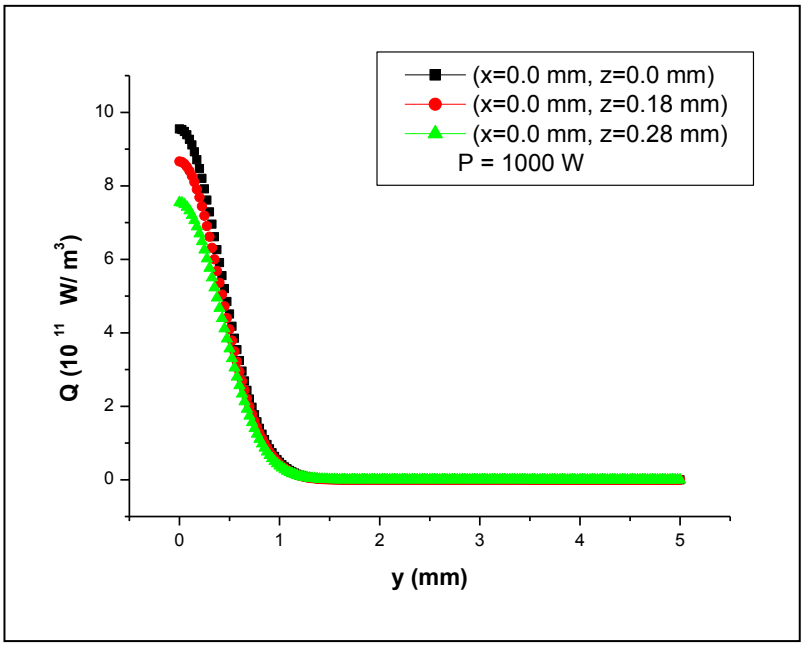

Figure III.2: Heat laser density according y.

2.2. Heat laser density according x

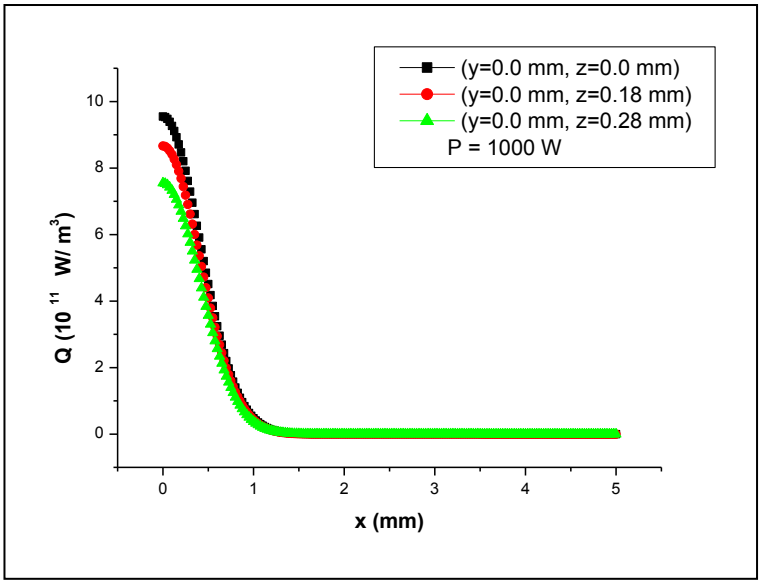

Figure III.3: Heat laser density according x

As expected, **Figure III.2** and **Figure III.3** show the symmetry of heat laser density with respect to axes x and y.

3. Profiles of temperature according time

Profiles of temperature according time are illustrates in **Figure III.4.**

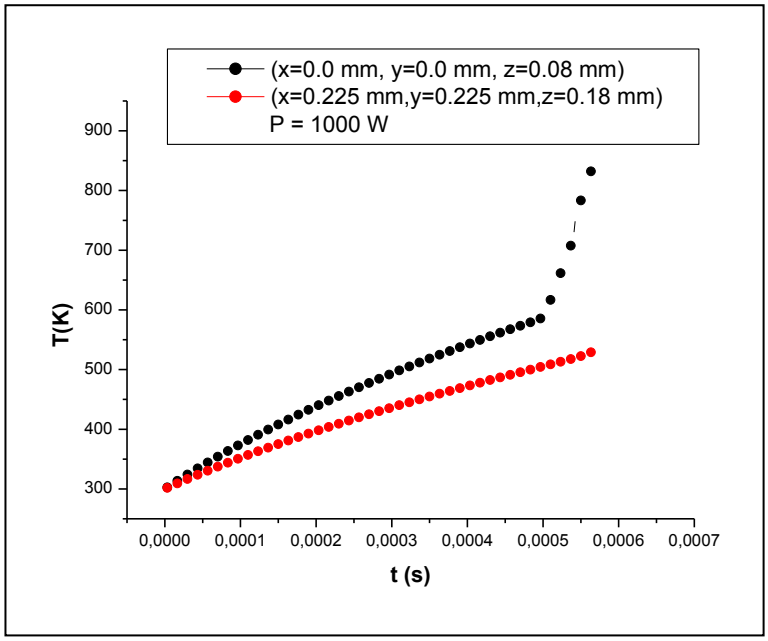

Figure III.4: Profiles of temperature as function of time, case of temperature depended properties

Results show a slow variation of temperature in solid phase compared to liquid phase and transition solid/liquid.

4. Profiles of temperature according position

Figure III.5, **Figure III.6 and Figure III.7** show the distribution of Temperature according position.

4.1. Temperatures according z

Figure III.5 gives temperature evolution as a function of the position z.

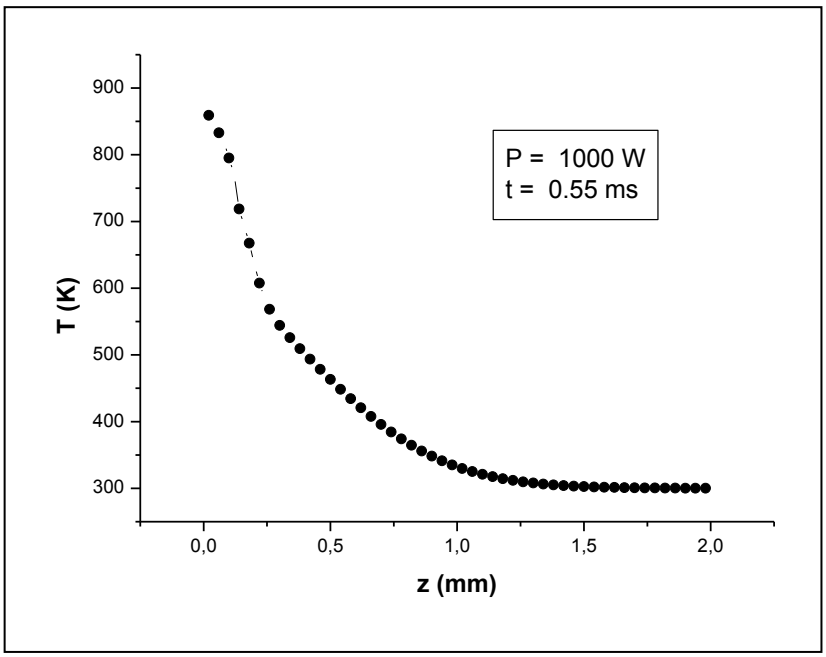

Figure III.5: Distribution of temperatures according z

4.2. Temperatures according x and y

Figure III.6 and **Figure III.6** present the variation of temperature as a function of the position x and y respectively.

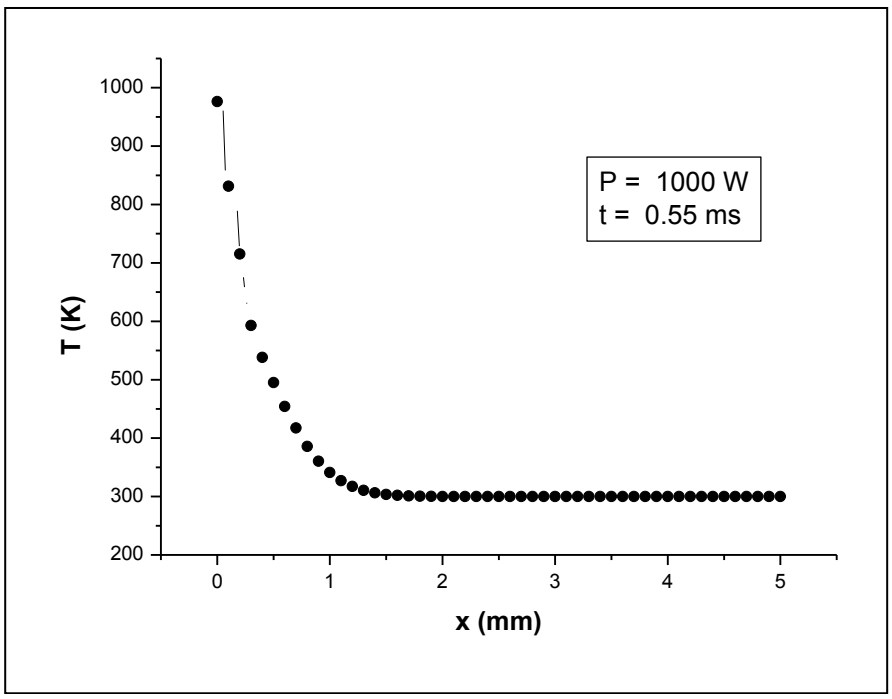

Figure III.6: Distribution of temperatures according x

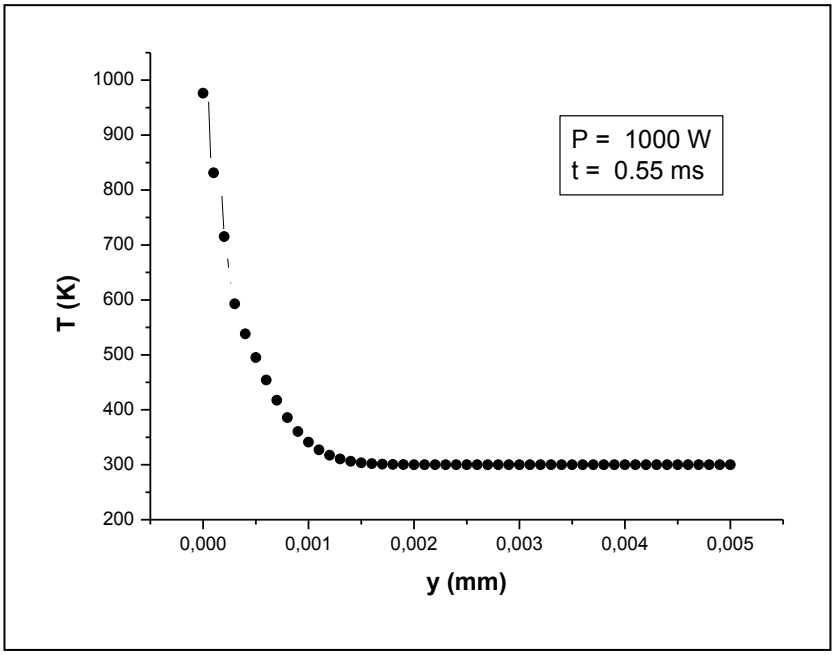

Figure III.7: Distribution of temperatures according y

It's noticed that the distribution of temperature increase when x, y and z decrease. In the farthest edge of the plate the temperature leads to initial temperature 300 K.

5. Temperatures according laser beam power

Distribution of temperature according x at the weld center for P=1000 W and P=1200 W is illustrates in **Figure III.8.**

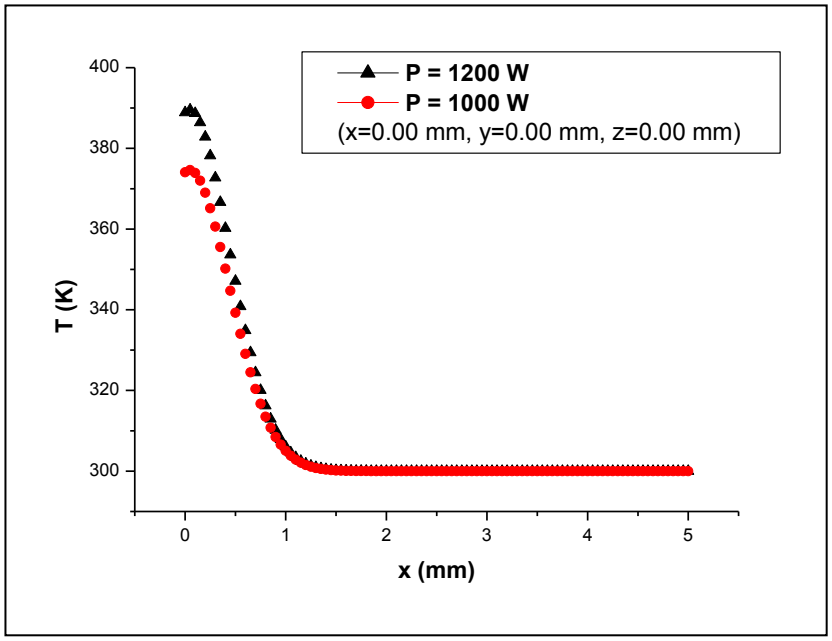

Figure III.8: Distribution of temperature according x at the weld center for P=1000 W and P=1200 W

Figure III.9 and **Figure III.10** give temperature evolution during laser welding at different positions (x = 0.0 mm, y = 0.0 mm, z=0.0 mm), (x = 0.225 mm, y = 0.225 mm, z=0.18), and on the weld bead for P = 800 W, P = 1000 W and P = 1200 W

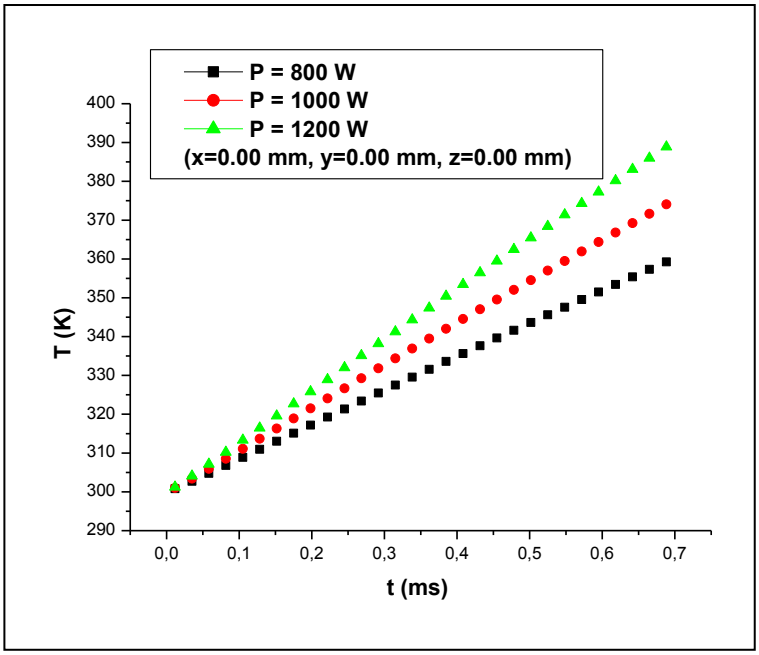

Figure III.9: Distribution of temperature as a function of time at the weld center for P=800W P=1000 W and P=1200 W

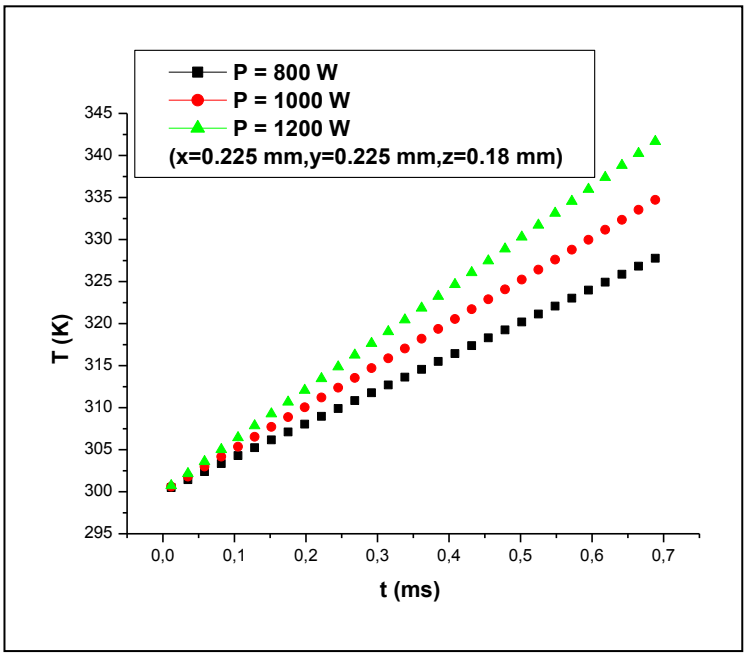

Figure III.10: Distribution of temperature as a function of time at (x = 0.225 mm, y=0.225 mm, z=0.18) for P=800W P=1000 W and P=1200 W.

Temperatures evolutions are proportional with laser beam power. This result is in accordance with those of [1-3].

6. Effect of thermal properties of the material

In this section, only the effect of thermal properties of the material (thermal conductivity, absorption coefficient, thermal capacity and density) is examined. In order to see the effect of these parameters, **Figure III.11** shows the effect of constant and variable density, thermal conductivity, and thermal capacity

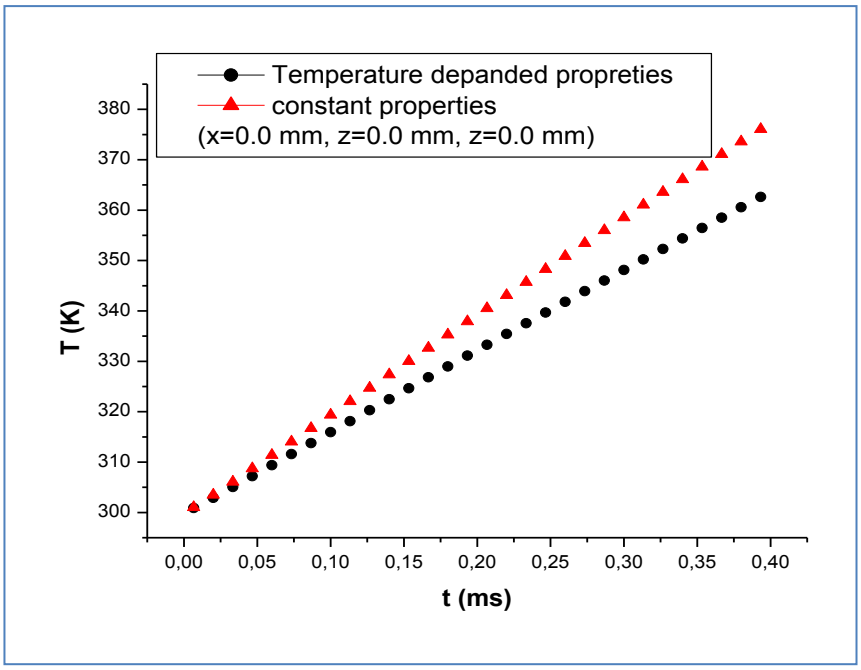

Figure III.11: Temperature profile with 1000 W laser power: comparison between constant and temperature depended properties.

It is seen that the results are close to each other with a small differences. The difference is observed when the temperatures increased. Therefore, it may be concluded that a constant material density value at room temperature can be used in numerical simulations to obtain temperature results for low temperatures.

7. Effect of convection and radiation losses on temperatures

It is necessary to take into account energy losses in the welding area to improve laser welding efficiency. These last need a calculation in the volume of materials, in and near the weld bead, with an appropriate formulation of the laser power. **Figure III.12** shows the amount of energy lost by convection and radiation according time.

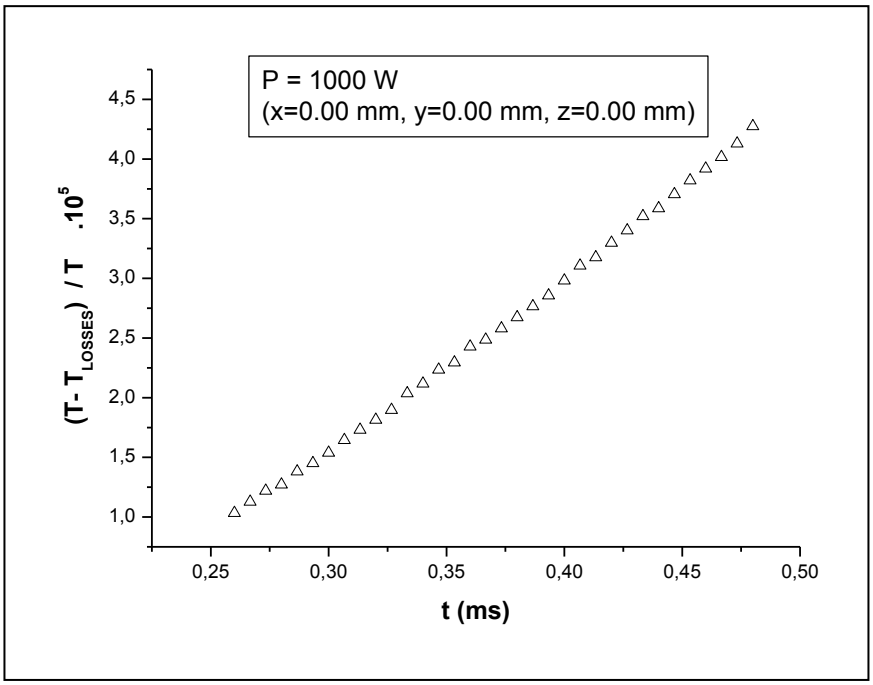

Figure III.12: The amount of energy lost by convection and radiation according time.

Under the welding conditions used in this study, variations in temperature $\Delta T/T$ did not exceed 0.01% for t_{max} = 0.001 s. **Table III.1** shows the temperatures changes with and without losses, as well as the ratio of the difference between them.

Table III.1: the amount of energy lost by convection and radiation according time.

t (10^{-1} ms)	$T(\sigma = 0, h = 0)$	$T'(\sigma \neq 0, h \neq 0)$	$\frac{\Delta T}{T}$ (10^{-3} %)
4,3	574,9802	574,9604	3,44
4,4	579,8478	579,8270	3,59
4,5	584,6699	584,6479	3,76
4,6	589,4471	589,4240	3,92
4.7	594,1726	594,1484	4,07

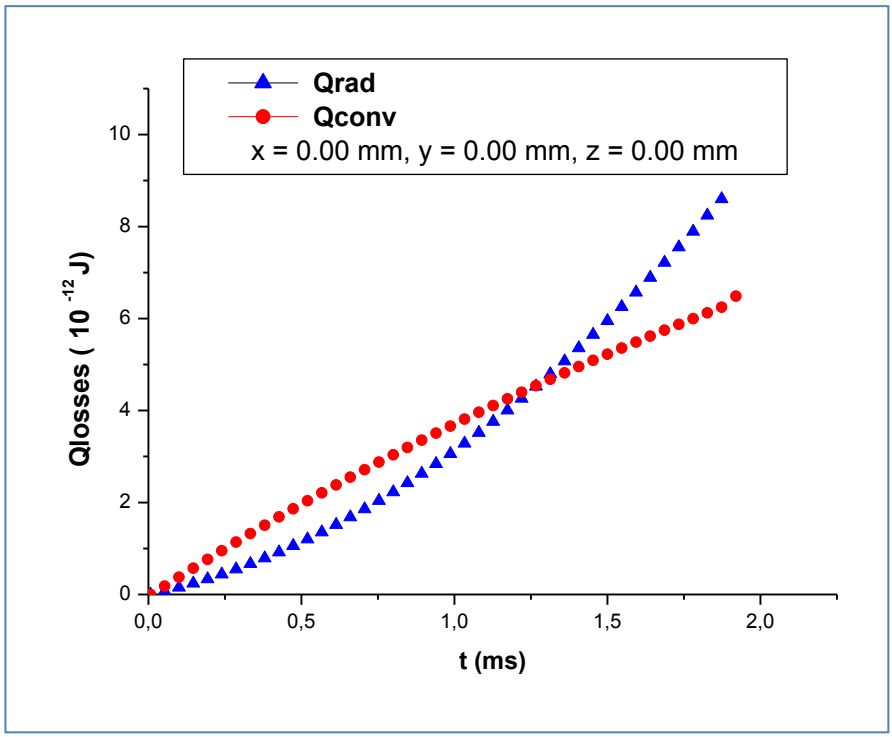

Figure III.13: The amount of energy lost by radiation and convection according time at the weld center

Figure III.13 shows the energy lost by radiation and convection in the weld center as function of time for P = 1000 W. It can be seen that during welding, the energy lost by radiation or convection varies according to time. The energy lost by radiation is less than to the energy lost by convection in [0 ms – 1.25 ms]. Then we see that the energy lost by convection is less than to the energy lost by radiation in [1.25 ms – 2 ms]. So there is a competition between the two phenomena radiation and convection.

8. Estimation of energy losses by evaporation

The surface illuminated by the laser beam becomes heated and then evaporates (The latent heat of evaporation is ten times more than the heat of melting). The majority of energy is transferred through conduction via solid material. Vaporization plays the secondary role in this case when the power density is less than 10^{10} W/m^2 [4].

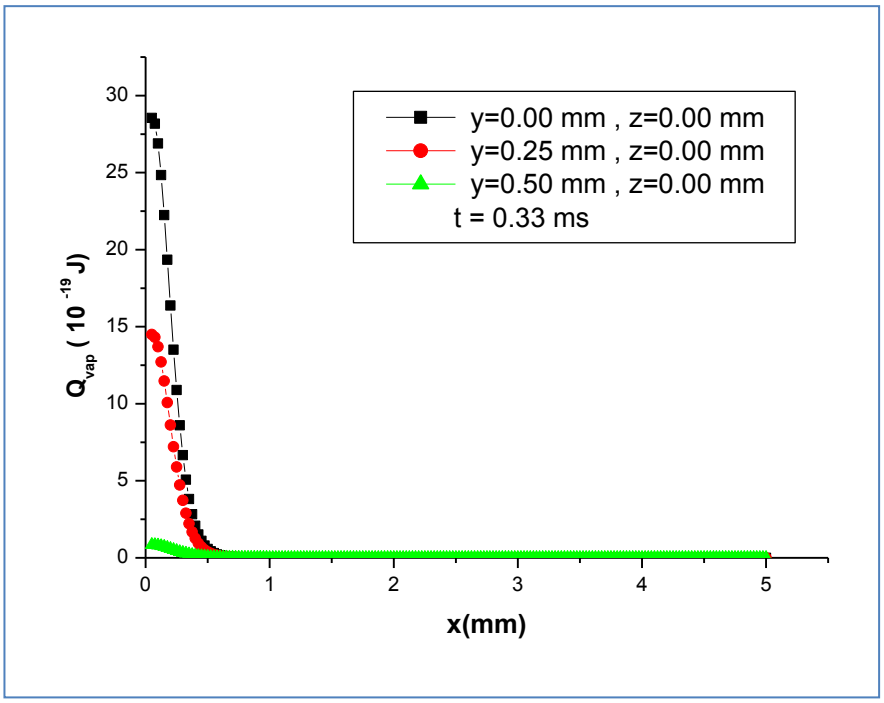

Figure III.14 : The amount of energy lost by evaporation according x at different position (y = 0.00 mm,z = 0.00 mm),(y = 0.25 mm,z=0.00 mm),(y = 0.50 mm,z=0.00 mm) at t=0.33 ms

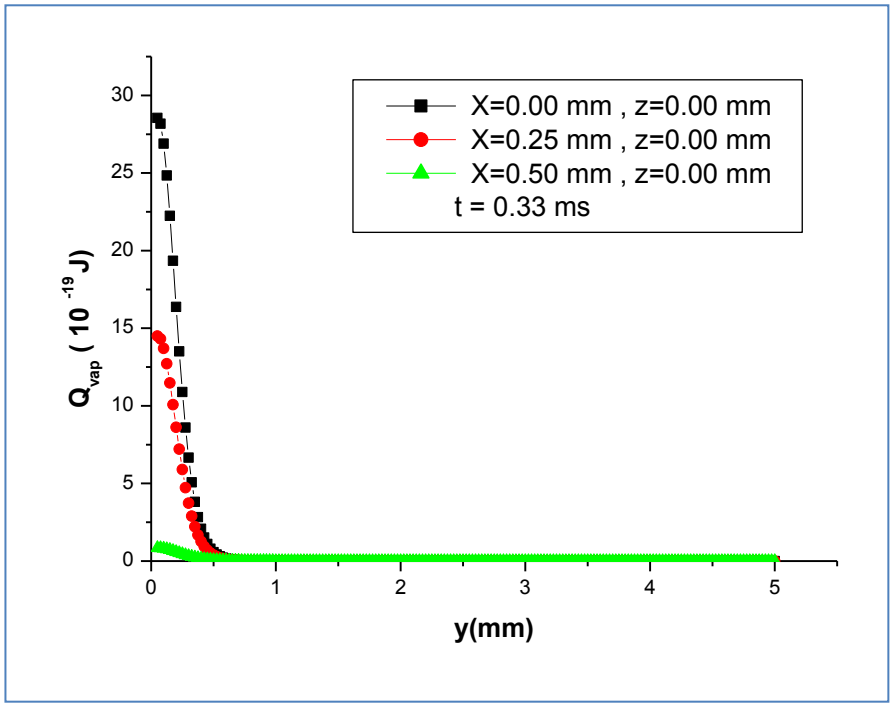

Figure III.15 : The amount of energy lost by evaporation according y at different position (x = 0.00 mm, z = 0.00 mm),(x = 0.25 mm, z = 0.00 mm),(x = 0.50 mm, z = 0.00 mm) at t=0.33 ms

It is clear that the energy lost near and on the weld center is greater than the energy lost in the rest of the plat.

9. Competition between different losses :

For the weld center, we obtained the following results:

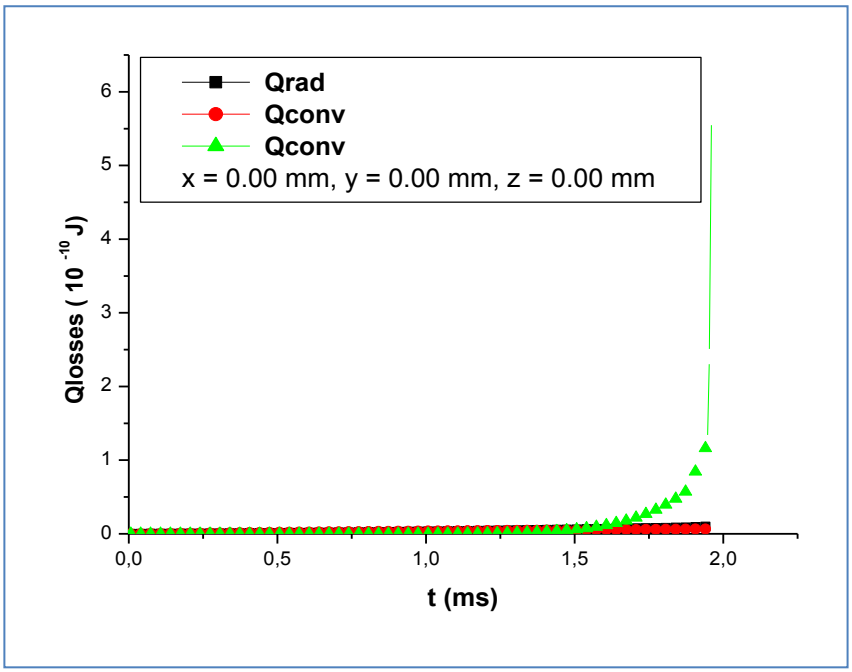

Figure III.16: Energy lost by convection, radiation and evaporation in the weld center as a function of time.

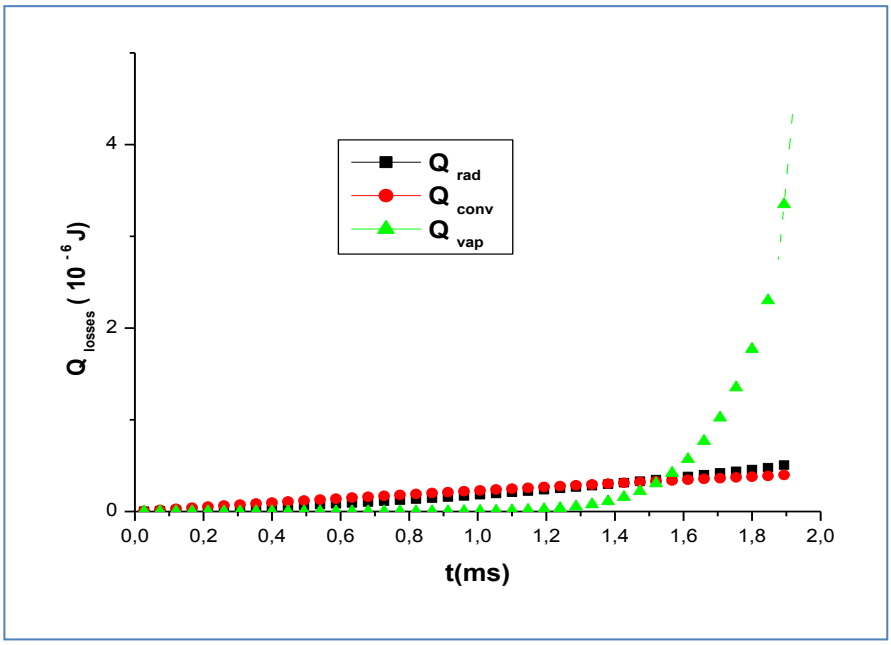

Figure III.17: Total energy lost by radiation, convection and evaporation as a function of time.

In **Figure III.17** we observed the following notes:

- for [0 ms – 1.5 ms] : total energy lost by evaporation is much less than total energy lost by radiation and convection.
- for [1.5 ms – 2 ms] : in this range of time, total energy lost by evaporation is greater than total energy lost by radiation and convection.
- The maximum value of energy lost by evaporation is about 5 10^{-6} J which is greater than the maximum value of energy lost by radiation and convection.
- The huge increase in the energy lost by evaporation may be explained by the occurrence of the phenomenon of keyhole formation or it may be due to errors in calculations.

10.The ratio of energy losses to laser beam energy :

The following figure shows the ratio between total energy lost by radiation, convection, evaporation and the energy of laser beam according time in the plate.

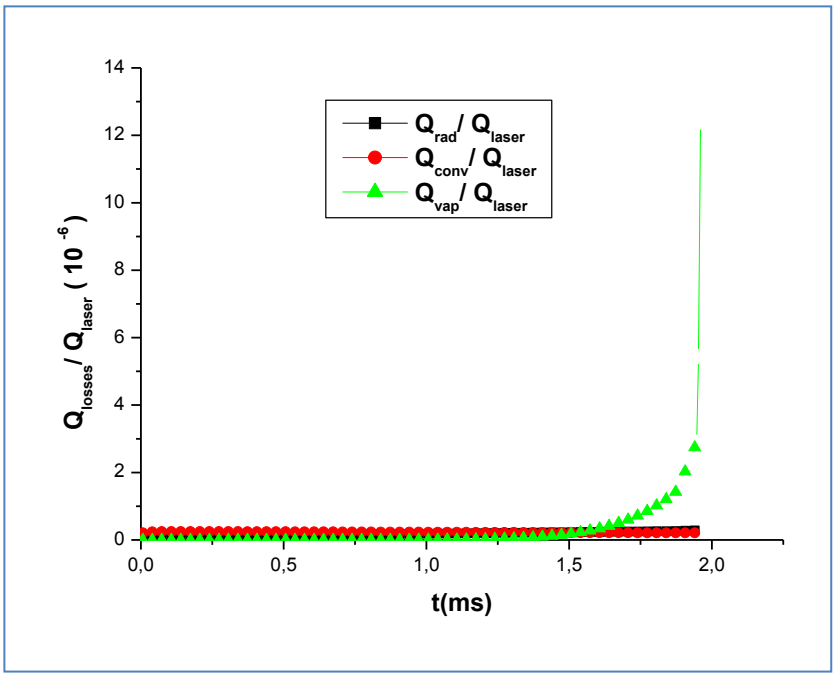

Figure III.18: The ratio between energy lost by radiation, convection, evaporation and the energy of laser beam according time in the plate.

Conclusion

As described above, a numerical study was developed in order to investigate the impact of heat source on metal alloy (AZ91). To achieve this study, a Gaussian volumetric heat source was proposed to model the incident laser beam power. A FORTRAN-based computer program was used for simulation.

We studied the variation of temperature and energy losses according position, power density and time. We found that:

→ The temperature increases when position x, y and z decrease and for the farthest edge of the plate it leads to initial value 300 K.

→ The temperatures evolutions are proportional with laser beam power.

→ Concerning the examination of the effect of thermal properties of the material on welding, we can say that a constant material properties value at room temperature can be used in numerical simulations to obtain temperature results for low temperatures.

→ The energy lost near and on the weld center is greater than the energy lost in the rest of the plat.

→ The huge increase in the energy lost by evaporation may be explained by the occurrence of the phenomenon of keyhole formation or it may be due to errors in calculations.

9. References

[1] S. Khemgani: Étude du rayonnement thermique lors de la soudure au Laser de plaques métalliques, Academic master, University of Ouargla, (2014).

[2] S. Benchaa: Répartition spatiale et temporelle d'énergie de sources lasers utilisées dans les dispositifs de soudage aux lasers de pièces d'alliages métalliques, Academic master, University of Ouargla, (2017).

[3] S. Lemkeddem, F. Khelfaoui, O. Babahani: Calculation of energy lost by radiation and convection during laser welding of TA6V titanium alloy, Journal of Theoretical and Applied Physics, 12(2), 113-120, (2018).

[4] J.Ronda, A. Siwek: Modelling of laser welding process in the phase of keyhole formation, archives of civil and mechanical engineering, 30, 30-059, (2011).

General conclusion and perspectives

Magnesium alloy are used widely in several fields. The AZ91 is one of the most used materials for laser welding due to its good mechanical and termophysical properties.

In this work we were interested in the study of a laser welding of tow symmetrical parts of the same alloy. A volumetric Gaussian heat power is applied on metal alloy.

In the first chapter, we presented basic notions of laser welding process. We mentioned basic equations.

In the second chapter we proposed a numerical modeling for laser welding of two identical parts. In order to calculate the temporal distribution of temperature, we suggested the resolution of the heat equation for solid and liquid phases and flow equation for phase transition solid/liquid, we considered the physical properties of material variable with temperature (heat capacity, specific heat and thermal conductivity). We took the system in three dimensions and none moving laser, the workpiece is also none moving. For the numerical modeling we applied Finite Differences Method (FDM) and iterative algorithm of Gauss-Seidel. We solved this problem in the presence of losses (by convection, radiation, evaporation)

In third chapter we present some results of simulation concerning the profile of heat source density according position and time and variations of temperatures in function of position and time. The effect of energy power and losses by convection and radiation on temperatures and temperature depended properties are presented. The results obtained showed that for high temperatures the effects of temperature depended properties and energy lost by radiation, convection and evaporation are considerable. For Laser welding of AZ91 during 2 ms with a power of 1000 W, we obtained a loss of energy by evaporation of 5.10^{-6} J while losses by radiation and evaporation are estimated to 4.10^{-5} J.

For perspectives, we suggest the following:

- Welding with mobile laser or mobile workpiece;
- Welding of non identical parts;
- The effect of other temperature dependent parameters (absorption coefficient, heat transfer coefficient.

Laser welding of metal alloy parts and calculation of losses by radiation, convection and evaporation

Abstract:

There are many industrial products made of assemblies of parts of magnesium alloy AZ91. There are also many scientific studies that have worked on this subject. In this work, we propose a 3D numerical model for the welding of two identical parts of AZ91 alloy, we used the heat equation to describe the energy distribution of solid and liquid phases and the flux equation for phase change. To solve these equations; the Finite Difference Method and the Gauss–Seidel method were used with a numerical program in FORTRAN language. The results obtained showed that for high temperatures the effects of temperature depended properties and energy lost by radiation, Convection and evaporation are considerable. Laser welding of AZ91 during 2 ms with a power of 1000 W gives a loss of energy by evaporation of 5.10^{-6} J while losses by radiation and evaporation are estimated about 4.10^{-5} J.

Keywords:

Laser welding, Heat equation, Numerical modeling, Convection, radiation, evaporation, magnesium alloy AZ91, Finite Difference Method, Gauss–Seidel Method.

Soudage laser des pièces métalliques et calcul des pertes par convection, rayonnement et vaporisation

Résumé:

Il existe de nombreux produits industriels qui sont constitués par des assemblages de pièces des alliages de magnésium AZ91 par soudage laser. Il existe également des études scientifiques qui ont travaillé sur ce sujet. Dans ce travail, nous avons proposés un modèle numérique 3D pour le soudage de deux pièces identiques d'alliage de AZ91, nous avons utilisé l'équation de chaleur pour décrire la distribution de l'énergie des phases solide et liquide et l'équation de flux pour le changement de phase. Pour résoudre ces équations. Les méthodes de différence finie et de Gauss–Seidel ont été utilisées à l'aide d'un programme numérique sous le langage FORTRAN. Les résultats obtenus ont montré que pour les températures élevées les effets de la dépendance des propriétés physique et des pertes sont considérables. Le soudage laser de AZ91 pendant 2 ms avec une puissance de 1000 W donne une perte d'énergie par évaporisation de 5.10^{-6} J alors que les pertes par rayonnement et convection sont estimées à environ 4.10^{-5} J.

Mots clefs :

Soudage laser, Équation de chaleur, Modélisation numérique, Convection, Radiation,evaporisation, alliages de magnésium AZ91, Méthode des Differences Finies, Méthode de Gauss–Seidel.

اللحام بالليزر للقطع معدنية و حساب الضياعات بالحمل، الإشعاع و التبخر

الملخص:

هناك عدة منتجات صناعية مكونة من تجميع قطع من سبائك المغنيزيوم AZ91 عن طريق اللحام بالليزر. كما أن هناك دراسات علمية عملت على هذا الموضوع. في هذا العمل اقترحنا نموذجا عدديا ثلاثي الأبعاد لنمذجة لحام قطعتين متطابقتين من سبائك AZ91، استخدمنا معادلة الحرارة لوصف توزيع الطاقة للطرين الصلب و السائل و معادلة التدفق للتغير في الطور. لحل هذه المعادلات تم استخدام طريق الفروق المنتهية و طريقة غوصايدل باستخدام برنامج عددي بلغة الفورترون. أظهرت النتائج التي تم التوصل لها أنه بالنسبة لدرجات الحرارة المرتفعة فإن تأثير استخدام خصائص المادة المتغيرة بدلالة درجة الحرارة و كذا تأثير الضياعات يكون معتبرا. لحام سبيكة AZ91 خلال 2ms بليزر إستطاعته 1000W أعطى طاقة ضائعة بالتبخر تقدر ب 5.10^{-6} J بينما قدرت الضياع بالإشعاع و التوصيل ب 4.10^{-5} J لكل منهما.

الكلمات الدالة:

اللحام بالليزر، معادلة الحرارة، النمذجة العددية، الحمل، الإشعاع، التبخر، سبيكة المغنيزيوم AZ91 ، طريقة الفروقات المنتهية، طريقة غوص -صايدال.